이학박사학위논문

Role of dorsomedial prefrontal cortex astrocytes in mouse dominance and depressive behavior

사회 서열행동 및 우울증에 미치는 전전두엽 성상교세포의 기능 연구

2020년 8월

서울대학교 대학원
치의과학과 신경생물학 전공

노 경 철

사회 서열행동 및 우울증에 미치는 전전두엽 성상교세포의 기능 연구

지도교수 이 성 중

이 논문을 이학박사 학위논문으로 제출함
2020년 7월

서울대학교 대학원
치의과학과 신경생물학 전공

노 경 철

노경철의 이학박사 학위논문을 인준함
2020년 7월

위 원 장 최 세 영 (인)

부 위 원 장 이 성 중 (인)

위 원 최 석 우 (인)

위 원 박 혜 윤 (인)

위 원 전 상 범 (인)

Abstract

Role of dorsomedial prefrontal cortex astrocytes in mouse dominance and depressive behavior

Kyungchul Noh

Program in Neuroscience
Department of Dental Science
The Graduate School of Seoul National University

Dominance behavior is a fundamental organizing mechanism for most animal societies. Achieving and remaining at a high social status are essential for survival. Recent studies have identified that pyramidal neurons in dorsomedial prefrontal cortex (dmPFC) region have a key role for remaining and maintaining at high social status. There is also a correlation between social status and mental health such as depression. In human, individuals with low socio-economic status (SES) are vulnerable to depression. Furthermore, astrocytes in dmPFC region are also involved in mouse depression and the response to anti-depressant drugs. Here, in this study, I suggest that dmPFC astrocytes in mice are directly involved in both dominance and depressive-like behaviors.

In the first part of this thesis, I applied both chemogenetic and optogenetic manipulation of dmPFC astrocytes into low social ranked mice. Both chemogenetic and optogenetic stimulation of dmPFC astrocyte successfully induced hierarchical rank graduation of subordinate mice by showing resistance behavior rather than pushing behavior during social competition. Optogenetic stimulation of dmPFC astrocytes increased extracellular glutamate level leading to the increase of excitatory synaptic inputs into layer V pyramidal neurons. I next compared astrocyte stimulation-induced dominance behavior with the results of neuron stimulation, and both mouse groups showed comparable winning rates in the tube test with different behavioral mode to achieve dominancy.

In the second part, I investigated the relationship between dominance behavior and depression. After 3 weeks of restraint stress (RS), the RS-received mice (RS mice) showed depressive-like behavior, and they also showed reduced dominance behavior compared with that of control mice. However, after chemogenetic stimulation of dmPFC astrocyte into RS mice, they showed increased resistance behavior against control mice during the tube test, and RS mice started to push, which was not observed during the basal behavior. This behavioral shift may be due to the prior winning experience obtained by resistance action, which might confer a winning effect. Furthermore, repetitive winning experience abrogated depressive-like behavior of RS mice. However, neuron-stimulated RS mice did not show anti-depressive behavior although they obtained winning experience by pushing action. This result suggests that rapid anti-depressive effect can be obtained by astrocyte-derived winning experience in mice.

In conclusion, dmPFC astrocyte activation enhances mouse dominance behavior by persistent resistance behavior. Moreover, depressive-like phenotype shown in chronic RS mice can be rapidly reversed by repetitive winning experience. This result suggests that the association between dominancy and depression through dmPFC astrocyte activity provides a clinical implication in treating depression due to low social status.

Key words: Dominance behavior, Astrocyte, Social hierarchy, Dorsomedial prefrontal cortex (dmPFC), Depression, Anti-depressant effect

Student Number: 2014-30697

Table of Contents

List of Figures

Chapter I. The role of dmPFC astrocytes in mouse dominance behavior

Chapter II. The effects of dmPFC astrocyte activation-induced dominancy on depression

Abbreviations

AAV	Adeno-associated virus
AAVDJ	Adeno-associated virus with serotype DJ
ACSF	Artificial cerebrospinal fluid
AMPA	alpha-amino-3-hydroxy-5-methyl-4-isoxazolepropionic acid
ArchT	Archaerhodopsin from *Halorubrum* TP009
ATP	Adenosine triphosphate
BBB	Blood brain barrier
BDNF	Brain-derived neurotrophic factor
CBT	Cognitive behavioral therapy
ChR2	Channelrhodopsin-2
CNO	Clozapine-N-oxide
CNS	Central nervous system
CRH	Corticotrophin releasing hormone
CSDS	Chronic social defeat stress
CUS	Chronic unpredictable stress
dmPFC	Dorsomedial prefrontal cortex
DREADD	Designer receptors exclusively activated by designer drug
DRN	Dorsal raphe nucleus
eHpHR	Enhanced halorhodopsin from *Natronomonas*
EPM	Elevated plus maze
EPSC	Excitatory post-synaptic current
FGF-2	Fibroblast growth factor-2
FST	Forced swim test
GABA	Gamma-aminobutyric acid
GDNF	Glial cell line-derived neurotrophic factor
GFAP	Glial fibrillary acidic protein
GPCR	G-protein coupled receptor

hM3Dq	Human M3 muscarinic receptor linked to the Gq protein
HRP	Horseradish peroxidase
L-AAA	L-alpha-aminoadipic acid
LTP	Long-term potentiation
MDD	Major depressive disorder
MDT	Mediodorsal thalamus
mEPSC	Miniature excitatory post-synaptic current
NA	Noradrenaline
NBQX	2,3-dioxo-6-nitro-7-sulfamoyl-benzo[f]quinoxaline
NeuN	Neuronal nuclei
NMDA	N-methyl-D-aspartate
NGF	Nerve growth factor
OFT	Open field test
PFC	Prefrontal cortex
PL	Prelimbic
RI	Resident intruder
RS	Restraint stress
S100β	S100-calcium-binding protein beta
sEPSC	Spontaneous excitatory post-synaptic current
SES	Socio-economic status
SSRI	Serotonin reuptake inhibitor
TrkB	Tropomyosin receptor kinase B
TST	Tail suspension test
VEGF	Vascular endothelial growth factor

Background and purpose

Background

1. Dominance behavior

1-1. Social hierarchy in human and animal

Human social status is prominent in different domestic, work, and recreational settings, where they define implicit expectations and actions that drive appropriate social behavior[1]. Furthermore, human social status predicts morbidity, survival, and even suicide[2-4]. A study has suggested an important role for hierarchical rank in achieving accurate self-knowledge and self-improvement, particularly in the usage of upward social comparisons[5]. Social hierarchies are usually emerged in children at age around 2 years[1,2]. Status within a social hierarchy is often made explicit, but can also be inferred from cues such as facial features, height, gender, and age[6]. In humans, dominance has been linked to heritable personality traits[7], because dominancy is also considered as a feeling of control and influence over one's surroundings or others versus feeling controlled or influenced by situations or others. Therefore, representing dominance behavior to reach high status in social hierarchy is an instinct behavior of human being.

Dominance behaviors can also be seen across various species of animal societies including fish[8], rodents[9,10], and monkeys[11,12], making this an instinctive behavior evolutionally preserved across the animal kingdom. According to the mouse studies, group-housed mice show stable social hierarchy[13,14]. These studies indicate that activity of neural population in dorsomedial prefrontal cortex (dmPFC) is a key mechanism related with social competition and winning[14]. Optogenetic neural potentiation of mediodorsal thalamus (MDT) and dmPFC

circuit is involved in the winner effect. Furthermore, dominance relationship can be predicted by initial social interaction[15]. Interbrain correlation measured by microendoscopic Ca^{2+} imaging technique is occurred when the two mice interact with each other. Result indicated that dominant mice preferentially drives interbrain synchrony, therefore, social dominant relationship can be predicted[15]. Considering that both human and other animals are all social species, developing hierarchy is natural phenomenon, and furthermore, trying to be a high social status is innate behavior.

1-2. Social status and health

As dominance hierarchies exist in numerous social species, and rank in such hierarchies can dramatically influence on the quality of an individual's life[16], social status can strongly influence on the health of an individual particularly in stress-related diseases. One factor that is pervasively linked to mood disorder is socio-economic status (SES), which is the evidence that individuals with low SES are affected by mental health problems and their adverse consequences[17,18]. Meta-analysis studies indicate that those of lower SES are at a higher risk of experiencing depression in their lifetime than those with high SES[19,20]. Low income, a gross marker of SES, has also been shown to be related to psychopathology, including suicidal ideation[21,22]. Indeed, although the absolute level of income is not a direct causal factor for mental health outcomes, however, the rank of income compared to others within a similar social group appears to be important[23,24]. These findings indicate that lower social status is associated with mental disorders.

The association between social hierarchy and mood disorders is also related with psychological feature such as emotion suppression[25]. Suppressing negative emotion has mental health cost, and individuals with low SES and low social status may use these strategies to avoid conflict[25]. It may be that it is not only the experience of negative emotion or lack of positive emotion that influences health, but the need to suppress the expression of emotion[26,27]. The experience of low social power and status unfolds in a social environment that may increase the need to suppress or inhibit one's experience to the extent that others with more power can punish and threaten them[28]. Moreover, facial muscle actions associated with the suppression of emotion are more common among individuals with low status compared to those with high status[29]. The process of silencing the self in order to maintain harmony within a social relationship is a proposed mechanism for the prevalence of mental health. These self-silencing is associated with emotion such as depression across individual's low SES in human.

Recent mouse studies suggested that dominant mice in social group exhibit aggressive behavior towards their cage mates and form a social hierarchy[13,14]. Dominant animals have different synaptic efficacies to subordinate animals[13]. Characteristic differences in gene expression in dominant and subordinate animals are also detectable. Dominant animals show higher expression of oestrogen receptor alpha, corticotropin releasing hormone (CRH) receptor 2, and androgen receptors in the nucleus accumbens and bed nucleus of the stria terminalis[30], which regulate social behavior and behavioral responses to stress. Brain-derived neurotrophic factor (BDNF), which is related to neural cell functions, including adult neurogenesis, is expressed more highly in the hippocampus of

dominant mice than subordinate mice[31]. These animal studies suggest that agonistic interactions between male mice alter neurological function in individuals kept under social conditions. Therefore, hierarchy in the mouse affects behavior and gene expression, resulting in mood disorder such as depression, and it is differently regulated in dominant and subordinate mice.

2. Depression

2-1. Overview of depression

Major depressive disorder (MDD) is the most common psychiatric disorder and is a leading cause of suicide[32]. MDD affects more than 300 million people worldwide in all age groups and has a higher frequency among other psychiatric disorders[33,34]. It is one of the leading causes of disability, which can induce suffering, reduce productivity, and negatively influence on social relationships[35,36]. Approximately 800,000 people die by suicide every year due to the depressive disorders[37,38], and it causes considerable damage to the economy such as the costs related to the treatment[39]. When associated with other pathologies such as cardiovascular, endocrine and pulmonary diseases, it increases mortality levels, besides the already high risk of suicide[40,41]. It is more prevalent in female, being two to three times more frequent in women than in men[39].

Stress is one major cause of onset of depression[42]. In particular, environmental factors are strongly influenced on the cause of depression in childhood[43]. People who grew up with the experience of maltreatment, physical punishment, family disruption such as parental divorce in childhood, and stressful

life are more likely to have poor mental health and depression[44]. Furthermore, children from socio-economically disadvantaged families are more likely to suffer from substance dependence and depression when they become an adult[44,45]. The number of adverse experiences also had a graded relationship to alcoholism and depression in adulthood[45].

A mouse study provided evidence of the existence of major differences in individual's susceptibility to stress[46-48]. Dominant individuals were the ones showing a strong susceptibility profile as indicated by strong social avoidance following chronic social defeat stress (CSDS), while subordinate mice were not affected. Furthermore, in subordinates rather than dominants, levels of these metabolites were increased after exposure to CSDS[47]. This study provide an insight that will facilitate progress on the identification of the neurobiological mechanisms inherent to vulnerability to stress and those that foster resilience.

Various brain regions are involved in depressive symptom. In particular, impaired function in the prefrontal cortex (PFC) region contributes to depression[49,50], and the therapeutic response produced by rapid-acting antidepressants such as ketamine are mediated by PFC activity[51,52]. Preclinical studies indicate that glutamatergic signaling in the dmPFC is critical to the therapeutic actions of ketamine[53]. A low dose of ketamine produces a paradoxical burst of glutamate in the mPFC, and neuronal silencing of the mPFC blocks the antidepressant actions of ketamine[53]. A key role for mPFC is also supported by optogenetic studies demonstrating that photostimulation of channelrhodopsin-2 (ChR2) expressing mPFC pyramidal neurons is sufficient to reproduce the rapid and sustained antidepressant behavioral actions of ketamine[52]. The dmPFC serves

as a central hub that can shape the activity in a distributed network of output structures, including regulation of behavioral and autonomic responses to stress.

2-2. Glial cells and depression

Astrocytes are arguably the most abundant glial cells in the central nervous system (CNS)[54]. In brain, astrocytes are the most abundant and versatile cells participating in most of brain functions[55,56]. Mounting evidence supports the contention that numerical and morphological alterations of astrocytes in the frontolimbic systems are closely associated with depression, as revealed in post-mortem studies of patients with MDD or suicide completers[57]. Astrocyte-specific markers such as glial fibrillary acidic protein (GFAP) and S100 calcium-binding protein β (S100β) have consistently yielded significant reductions in the number and density of astrocytes in the PFC[58,59]. These reductions are paralleled by astrocyte hypotrophy, that is, shrinkage of the size of GFAP-expressing cell bodies and processes in younger patients with MDD. In particular, the expression levels of the GFAP gene and protein are consistently decreased in the PFC[58,60].

One of the most consistent findings in postmortem studies of MDD patients is a decrease in the density and number of astrocytes, as well as reduction in the size of neuronal cell bodies, in cortical regions of dmPFC[58,61]. The decreases in glial density are accompanied by a reduction of astrocytic markers, such as GFAP[61]. These observations indicate that glial alterations in the dmPFC contribute to depressive symptom[58], which is a consequence or cause of the illness. A mouse

study provided the evidence of astrocyte loss in the dmPFC is sufficient to induce depressive-like behavior of rodent[58]. According to this study, L-α-aminoadipic acid (L-AAA) was infused into dmPFC. After L-AAA infusions, it induced decrease the density of astrocytes in the prelimbic cortex of dmPFC region, and provoked a reduction of dendritic length and complexity of the processes of GFAP-positive cells, suggesting astrocytic atrophy. L-AAA infusion into dmPFC region also induced anhedonia, anxiety, and depressive-like behavior in rats[60]. These behaviors were similar to those who received chronic unpredictable stress (CUS)[62].

Findings from clinical and preclinical studies suggest that astrocyte pathology may be a potential contributor to the pathophysiology and pathogenesis of major depression[57,63]. Many other astrocytic functions are altered in MDD, including ion and water homeostasis[64], γ-aminobutyric acid (GABA) and monoamine recycling[65], blood brain barrier (BBB) integrity[66], gliogenesis[67], and synaptogenesis[68]. Most of these alterations target anti-depressants. These suggest that MDD is considered as a disease of astrocyte pathology, and highlight previous studies on promising strategies that direct target of astrocytes for the development of novel antidepressant treatments.

2-3. Therapeutic trials for depression

Antidepressants are a class of drugs that reduce symptoms of depressive disorders by correcting chemical imbalances of neurotransmitters in the brain[69,70]. Chemical imbalances may be responsible for changes in mood and behavior. Neurotransmitters are vital, as they are the communication link between neuronal

cells in the brain. The prevalent neurotransmitters in the brain specific to depression are serotonin[71,72], dopamine[73,74], and norepinephrine[75,76]. In general, antidepressants work by inhibiting the reuptake of specific neurotransmitters, hence increasing their levels around the synapses within the brain, such as selective serotonin reuptake inhibitors (SSRIs), antidepressants that will affect serotonin levels in the brain.

Most antidepressants increase the extracellular serotonin or noradrenaline (NA) levels by inhibiting the reuptake of monoamine in presynaptic terminals. Although changes in extracellular monoamine levels occur soon after the drug administration, the clinical antidepressant effect develops slowly over several weeks of continuous treatment[77]. Clinical and animal studies have suggested that several neurotrophic/growth factors play important roles in the efficacy of anti-depressant, which is assumed to be associated with neuronal plasticity, such as neurogenesis and synaptogenesis[78-80]. Clinical studies have indicated that lower levels of fibroblast growth factor-2 (FGF-2), BDNF, and glial cell line-derived neurotrophic factor (GDNF) in the postmortem brain or blood from patients with MDD were attenuated by antidepressant medications[77,81]. Animal studies have shown that FGF-2, BDNF, and vascular endothelial growth factor (VEGF) were induced by antidepressant treatment in several brain regions[82], and the administration of FGF-2, BDNF, VEGF, and nerve growth factor (NGF) to rodents produced antidepressant-like effects[81].

These neurotrophic/growth factors are produced not only in neurons, but also in astrocytes[77,83]. Astrocytes have monoaminergic receptors, and regulate the production of neurotrophic/growth factors including FGF-2, BDNF, GDNF and

NGF through the activation of monoaminergic receptors[84]. These findings suggest that astrocytes, as well as neurons, play important roles for the regulation of neurotrophic/growth factors by antidepressants in the brain. These reports suggest a novel concept that antidepressants directly act on astrocytes.

Although several effective treatment of anti-depressants, it is estimated that one-third of depressed patients do not respond adequately to conventional antidepressant drugs[85,86]. Moreover, not only the slow onset of their therapeutic effects also restricts antidepressant use [87,88] but also side effects exist when using the drugs[89,90].

3. In vivo manipulation

Optogenetics is a novel biological technique based on a variety of light-sensitive proteins called opsins, which include microbial ion channels and ion pumps as well as engineered G-protein coupled receptor (GPCR)[91,92]. Following absorption of a specific wavelength of light, an opsin undergoes a conformational change that triggers diverse cellular changes in opsin-expressing cells. Some of the opsins induce the translocation of ions, and others activate intracellular signaling cascades, such as G protein-mediated signaling. Since most of these opsins do not exist in experimental-model organisms, and photostimulation itself has a negligible effect on cells and tissues, optogenetics has instead been used as a powerful experimental tool to manipulate specific populations of cells both in vitro and in vivo by means of a combinatorial approach of cell type-specific promoters and additional genetic tricks. This technique has also enabled the manipulation of

cellular activity with millisecond-scale temporal precision[91]. The timeresolved stimulation has made possible the revelation of causal relationships between manipulated cellular activity and functional outcomes, particularly in the study of neuronal circuits mediating specific behaviors.

There are several opsins which can be utilized for the manipulation of neuron cells such as ChR2, halorhodopsin (eNpHR), and archaerhodopsin (ArchT). Among those opsins, channelrhodopsin, originally identified in green algae, is a cation channel that becomes permeable to positively charged ions such as proton and sodium when it is stimulated with blue light[93-95]. When it is expressed in neurons, 473 nm light elicits an influx of cations, which causes depolarization and the firing of action potentials in the stimulated cells[91].

Chemogenetics is based on engineered proteins, such as GPCRs and ligand-gated ion channels, that are no longer responsive or only very weakly responsive to their endogenous ligands but strongly respond to synthetic chemical ligands that are otherwise biologically inert[96-98]. For example, hM3Dq, one of the designer receptors exclusively activated by designer drugs (DREADDs), is generated by multiple cycles of randomized mutagenesis of the human M3 muscarinic receptor, which is linked to the Gq protein[99]. It is neither sensitive to the endogenous muscarinic acetylcholine receptor ligand acetylcholine nor is it constitutively active, but it is strongly activated in response to a synthetic ligand, clozapine-N-oxide (CNO), with nanomolar potency[96]. In response to CNO, hM3Dq can induce an enhancement of neuronal excitability that can lead to burst-like firing[100,101]. Thus, it is one of the most frequently used chemogenetic tools to activate cells.

Purpose

Social status is crucial for maintain individual's life and mental health. Individuals with low social status are more vulnerable to psychiatric disorder such as depression. Recent study revealed that mouse social hierarchy is directly modulated by the layer V pyramidal neurons in dmPFC. Although increasing evidence indicate that neural activation is affected by nearby glial cells such as astrocyte, the role of astrocyte in the relation between dominance and depression is unknown. In this study, I tried to elucidate the involvement of dmPFC astrocyte in mouse dominance and depressive behaviors. To do this, I tried to series of experiments with the following specific aims:

1. To elucidate the role of dmPFC astrocyte in mouse social dominance behavior.
2. To find the effects of dmPFC astrocyte activation-induced dominancy on depression.

The research on the above specific aims is addressed in subsequent two chapters.

Chapter I

The role of dmPFC astrocytes in mouse dominance behavior

Abstract

Dominance behavior is an instinct behavior for survival in animal society. Recent study have indicated that neural activation in the dorsomedial prefrontal cortex (dmPFC) is implicated in the graduation and maintenance of dominance hierarchies. However, although increasing evidences show that astrocytes can directly affect neural activity, the role of astrocytes in dominance behavior has not been investigated. In this regard, I investigated the role of dmPFC astrocyte in mouse dominance behavior.

Both chemogenetic and optogenetic astrocyte activation enhanced excitatory synaptic inputs of layer V pyramidal neurons of the dmPFC by glutamate release without affecting neuronal excitability. Such dmPFC astrocyte activation in subordinate mice induced both a hierarchical rank increase by increasing the persistence of defensive behavior. As a mechanism, increased extracellular glutamate was observed after optogenetic dmPFC astrocyte stimulation. Also, surface AMPA receptor expression correlated miniature excitatory postsynaptic current (mEPSC) amplitude after rank elevation of rank-4 mice.

In this chapter, data show that social dominance can be manipulated by dmPFC astrocyte via glutamate release. The results suggest a novel behavioral strategy to change social rank.

Key words: Social hierarchy, Dominance behavior, Astrocyte, Dorsomedial prefrontal cortex (dmPFC), Glutamate, AMPA receptor

Introduction

Social hierarchy is a naturally occurring and evolutionarily conserved instinct phenomenon that serves as a guiding principle for the access to resources such as food, mating probabilities and resting spots[102,103]. Achieving and remaining at a high social status are essential for survival in both human and animal society. Moreover, it has profound influences on health and disease in both animals and humans[104]. There is a strong correlation between social status and psychiatric conditions; those with lower social status are more vulnerable to depression due to social defeat from others, while those with high social status have greater self-esteem and psychological health[3,23]. Efforts to reach a higher social status and maintain it in animal society are represented by dominance behavior such as offensive action and resistance to opponents. Such dominance behaviors can be seen across various species[13,105,106], making this an instinctive behavior evolutionally preserved across the animal kingdom.

The establishment of social dominance relies on the well-organization and orchestration of multiple brain regions such as dorsomedial prefrontal cortex (dmPFC), hippocampus, amygdala and nucleus accumbens[107]. Among them, recent studies show that the dmPFC is a key neural substrate controlling mouse dominance behavior[13,14]. Specifically, the strength of synaptic input to dmPFC layer V pyramidal neurons correlates with dominance behavior and social rank[13]. Also, ablation of BDNF/Tropomyosin receptor kinase B (TrkB) signals in the inhibitory neurons increases social dominance, which is reversed by optogenetic silencing of the excitatory neurons in the dmPFC[108]. Furthermore, repetitive

winning experiences of mice in tube tests potentiates synaptic activity of the mediodorsal thalamus (MDT) to the dmPFC circuit, which is necessary and sufficient for the maintenance of dominance hierarchy in mice[14]. Accordingly, how to potentiate the synaptic activity of dmPFC neurons is the key issue in maintaining dominance in social hierarchies and achieving the 'winner effect'.

Pioneering studies indicate that astrocytes, a component of the tripartite synapse, play a critical role in regulating synaptic activity. Chemogenetic astrocyte activation induces *de novo* long-term potentiation (LTP) in the Schaffer collateral pathway of the hippocampus[109]. In addition, spinal cord astrocyte activation causes gliogenic LTP at synapses between C-fibers and lamina I neurons of the spinal cord[110]. Therefore, astrocytes can induce and maintain neuronal synaptic potentiation via various gliotransmitters[111-113]. In addition, increasing evidence supports that astrocytes can directly affect mouse behaviors by regulating synaptic transmission between pre- and post-synaptic neurons[114,115]. For instance, hippocampal astrocytes modulate mouse memory performance by affecting NMDA-dependent long-term potentiation[109] and long-term depression[116] in the hippocampal CA1 region. Likewise, astrocytes in the hypothalamic arcuate nucleus inhibit food uptake by inactivating agouti-related peptide neurons via adenosine A1 receptors[117]. However, although astrocyte cell in brain can directly affect and change various mouse behaviors, it is still unknown whether mouse dominance behavior is affected by astrocyte. Specific regulatory mechanisms of such astrocyte-regulated mouse behaviors are different depending on the brain sub-regions involved, however, regulation of synaptic transmission of each neural circuit responsible for the behaviors by astrocyte-derived gliotransmitters has been

suggested as a common denominating mechanism[118,119]. Therefore, given such a role for astrocytes, it is conceivable that astrocyte activity may influence the dominance hierarchy of mice by the effects on dmPFC synaptic activity. Here, I explored whether mouse dominance hierarchy could be manipulated by chemogenetic and optogenetic activation of dmPFC astrocytes.

Materials and Methods

Animals

Six to 16-week-old male C57BL/6J mice of similar body weights were used for experiments. The animals were housed and maintained in a controlled environment at 22-24°C and 55% humidity with 12 h light/dark cycles and fed regular rodent chow and tap water ad libitum. All animal care was guided by the Seoul National University Institutional Animal Care and Use Committee (SNU IACUC, SNU-180416-3).

Stereotaxic Viral delivery

Nine to 10-week-old wild type male mice that showed stable hierarchy in cages were used for viral delivery. Animals were anesthetized with isoflurane and secured in a stereotaxic frame (Stoelting Co., Wood Dale, IL, USA). Holes the size of the injection needle were drilled into the skull, and bilateral or unilateral injections with 0.7 μl (titer 10^{13} GC/ml) of adeno-associated virus with serotype DJ (AAVDJ) were administered in each side. The injection syringe (Hamilton Company, Reno, NV, USA) delivered the AAVDJ at a constant volume of 0.1 μl/min using a syringe pump (Stoelting Co.). The needle was left in place for 3 min after each injection to minimize the upward flow of the viral solution after raising the needle. The injection coordinates of the prelimbic (PL) cortex of the dmPFC were angle: 10°, AP: +2.43, ML: ±0.61, DV: -1.78 from bregma. Mono fiber-optic cannula were bilaterally implanted 1 week after the viral injection, 400 μm above the viral injection site (angle: 10°, AP: +2.43, ML: ±0.61, DV: -1.38 from bregma). Anchor

screws were located in the skull and fixed with Zinc Polycarboxylate dental cement. AAVDJ-GFAP-mCherry, AAVDJ-GFAP-ChR2-mCherry, AAVDJ-hSyn1-mCherry, and AAVDJ-hSyn1-ChR2-mCherry were purchased from the Korea Institute of Science and Technology (KIST, Seoul, Korea). Animals injected with virus were used for assessments of behaviors 3 weeks after the injection. Animals injected with AAVDJ but showing no detectable viral expression in the target region were excluded from the analyses.

Simultaneous stereotaxic implantation of optic fiber and guide cannula

To assess AMPA or NMDA-receptor mediated dominance behavior, both a guide cannula (Plastic1, Roanoke, VA, USA) and mono fiber-optic cannula were implanted in the same region simultaneously. With the identical stereotaxic procedure mentioned above, we implanted a guide cannula (C315GMN) covered by its dummy (C315CMN) (angle: -10°, AP: +2.43, ML: 0.01, DV: -1.58 from bregma) and a mono fiber-optic cannula (angle: +20°, AP: +2.43, ML: +0.94, DV: -1.46 from bregma) to target the right dmPFC. The end of the guide cannula was 200 μm above, and optic fiber was 400 μm above the target region. To perform *in vivo* microdialysis, we simultaneously implanted both a CMA7 guide cannula (CMA Microdialysis, CMAP000137, Kista, Sweden) (angle: -10°, AP: +2.43, ML: 0.01, DV: -1.58 from bregma) and a mono fiber-optic cannula (angle: +20°, AP: +2.43, ML: +0.94, DV: -1.46 from bregma) with an identical procedure as described above.

Behavioral studies

On the day of all behavioral testing, animals were moved to the test room and left to habituate for at least 1 h. The light condition of the test room was maintained at the same intensity (100 lux) as the animal rooms under daylight conditions.

Tube test. The tube test was conducted as described [120]. We used a transparent Plexiglas tube with 30 cm length and 3 cm inner diameter. Six-week-old male mice were housed in groups of 4 for at least 2 weeks before tube test. Before the main test, each mouse was trained to go through the tube for 10 trials in two consecutive days. On the test day, pairs of mice were released into the opposite ends and met at the middle of the tube. The tube test was performed for 2 min. If no winner or loser was decided within 2 min, the test was repeated. Between each trial, the tube was cleaned with 70% ethanol. Within each cage of four pairs, mice were randomly assigned such that each mouse would meet every other mouse of the group only once, resulting in six matches per cage. All 6 pairs of mice were tested daily with a round robin design and ranks were determined by total number of wins. Only cage mates that maintained stable ranks for at least 3 or 4 days were used for further experiments. The behaviors were videotaped and both push and resistance behaviors were counted.

Tube test with optogenetic stimulation. We used optogenetic manipulation of dmPFC astrocytes and neurons in mice implanted with a mono fiber-optic cannula expressing ChR2 in astrocytes or neurons, respectively. We used 200 μm optic fibers (Thorlabs Inc., FP200URT, Neuton, NJ, USA) with a 1.25 mm ceramic ferrule (Thorlabs Inc., CFLC230-10) for bilateral stimulation and 300 μm optic fibers (Thorlabs Inc., FT300EMT) with 2.5 mm ceramic ferrules (Thorlabs Inc., CF340-10) for unilateral stimulation. We considered only cage mates with a stable

tube test rank for at least 3 or 4 consecutive days, and all four mice were implanted with an optic fiber in the dmPFC region. We used a tube opened with a 1.2 cm slit at the top of the tube. All four mice were habituated to the fiber connection and tested in the tube with fake optic fibers for 3 days before the main experiment. On test day, in the mice expressing AAVDJ-GFAP-ChR2-mCherry (GFAP-ChR2 mice), 473 nm blue light delivery (20 Hz, 25 ms of pulse duration) (Shanghai Laser & Optic Century, Shanghai, China) was applied 20~30 seconds before mice entered the tube. In the mice expressing AAVDJ-hSyn1-ChR2-mCherry (hSyn1-ChR2 mice), the blue light was applied right before entering the tube. Optogenetically stimulated rank-4 mice were matched with rank-3 mice first, and then with mice with a larger rank difference, namely rank-2 and rank-1 mice. If rank changed in the tube test, we switched the mouse pair to the opposite sides of the tube and repeated the test. We considered a rank change successful only when the rank-4 mice won from both sides of the tube. We applied light intensity of around 1 ~ 10 mW.

Dominance competition between the mice expressing neuronal ChR2 and astrocytic ChR2. We first measured the winning rate of each test mouse (GFAP-ChR2 and hSyn1-ChR2 mice) competing with their matched control (expressing AAVDJ-GFAP-mCherry or AAVDJ-hSyn1-mCherry). All control and test mice were individually housed for at least two weeks to avoid dominancy among the cage mates. On the test day, after 2 days of tube training, each test mouse was matched against 10 control mice, and the winning rates of all test mice were averaged. We next compared dominance competition between the mice with neuronal and astrocytic ChR2 activation (473 nm, 20 Hz, 25 ms of pulse duration).

The mice from each group were randomly paired with the mice from the other group, and the winner was determined when one mouse won twice out of three tests (best of three). Different mice sets were used for the two experiments.

Tube test with optogenetic astrocyte stimulation delivering NBQX and vehicle. We delivered NBQX (10 μM) *via* guide cannulas (C315GMN, Plastic1) 30 min prior to the tube test [121]. In the tube test, light stimulation (473 nm, 20 Hz, 25 ms of pulse duration) was provided only to rank-4 mice. Optic stimulation was provided only 0.5 h after drug delivery and the behavior test was performed at various time points (0.5, 1.5, 3, and 24 h after drug delivery).

Resident-intruder test. A resident-intruder test was applied by modifying the method to detect reliable aggressiveness of C57BL/6J male mice[122]. Male and female mice were co-housed together for at least 3-4 weeks before the main test. On the test day, the female mouse was removed from the cage and a new, 1-week younger C57BL/6J male mouse was introduced as an intruder for 10 min. The behaviors of the residents with or without light stimulation (473 nm, 20 Hz, 25 ms of pulse duration) were videotaped for analysis. Aggressive behaviors such as chasing duration, attack frequency, and attack duration were counted.

Open field test (OFT). The apparatus consisted of a brightly illuminated 40 cm x 40 cm square arena surrounded by a 40 cm high wall. Mice were individually placed in the center of the arena, and their locomotion activity was monitored by an automatic system for 10 min. Light stimulation of 473 nm was intermittently turned on and off on the test mice (GFAP-ChR2 mice and GFAP-mCherry mice) with 1 min intervals. Total distance and time spent in the center zone per minute were analyzed by automated video tracking system (SMART, Panlab SL,

Barcelona, Spain). The activity chamber was cleaned with 70% ethanol after each use to eliminate any olfactory cues from the previously tested mouse.

Elevated plus maze (EPM). The behavioral apparatus consisted of two open arms (width 5 cm x length 30 cm) and two closed arms (width 5 cm x length 30 cm) elevated 60 cm above the floor and dimly illuminated. Mice were placed individually in the center of the maze facing an open arm and allowed to freely explore for 5 min. Light was delivered during the whole experimental session to GFAP-ChR2 mice and their control group. The time spent in each arm was analyzed using a video tracking system. The maze was cleaned with 70% ethanol after each test to prevent influence from the previously tested mouse.

Forced swim test (FST). We conducted forced swim tests by placing each animal individually in transparent cylinders filled with water (23-25°C; depth 15 cm) for 5 min. Immobility in the FST was defined as the state in which mice were judged to be making only the movements necessary to keep their head above the surface. Light was delivered during the whole experimental session to GFAP-ChR2 mice and their control group. Both trials were videotaped and immobility time was analyzed using a video tracking system.

Experimental protocols including OFT, EPM, and FST were designed to take into account potential stress that could affect test mice behavior[123]. After the tube test, behavioral assessment was performed in the following sequential order to minimize stress effects: OFT, EPM, and FST. We performed each behavior test at least 48 h after the previous test to minimize potential stress effects.

OFT, EPM, and FST with treatment of NBQX or vehicle. We stereotactically implanted both an optic fiber and guide cannula simultaneously into the dmPFC

region. Three days after the surgery, we performed behavior tests 30 min after drug delivery *via* guide cannula. NBQX (10 μM) were delivered at a volume of 1 μl at a rate of 0.5 μl/min. Each behavior was tested at least 48 h after the previous test to minimize potential stress effects.

Primary astrocyte culture and in vitro Ca^{2+} assay

Primary astrocytes were isolated from the hippocampus and cortex of postnatal day 1 mice and prepared using a modified established protocol[124]. Briefly, after removing the meninges from the cerebral hemisphere, the tissue was dissociated into a single-cell suspension by gentle repetitive pipetting and filtered through a 70 μm filter. The cells were cultured in DMEM supplemented with 10 mM HEPES, 10% FBS, 2 mM L-glutamine, and 1X antibiotic/antimycotic in 75 cm^2 flasks at 37°C in a 5% CO_2 incubator. The medium was changed every 5 days. After 2 weeks, the flask was shaken at 250 rpm for 2 h at 37°C, treated with 100 mM L-leucine methyl ester for 60 min to remove the microglial cells, and harvested using trypsinization (0.25% trypsin, 0.02% EDTA). Calcium response in astrocytes expressed ChR2 was measured by single-cell calcium imaging using Rhod-2AM (Invitrogen, Carlsbad, CA, USA). Primary cells were plated on PDL-coated cover glasses and incubated overnight. Cells were incubated for 50 min at 37°C with 2 μM Rhod-2AM in HBSS containing 25 mM HEPES (pH 7.5) and washed with HBSS-HEPES twice before assays. A baseline reading was taken for 100 sec before blue light (473 nm, 20 Hz, 25 ms) stimulation. Intracellular calcium levels were measured by digital video microfluorometry with an intensified charge-coupled device camera (CasCade, Roper Scientific, Trenton, NJ, USA) coupled to

a microscope and analyzed with MetaFluor software (Universal Imaging Corp., Downington, PA, USA). Increases in the fluorescence intensity over baseline were calculated for each trace and are reported as $\Delta F/F_0$.

Immunohistochemistry

The whole brain was saline-perfused, fixed in 4% paraformaldehyde in 0.1 M PBS overnight at 4°C, and dehydrated with 30% sucrose for 3 days. Coronal sections with a thickness of 50 μm were incubated in cryopreservation solution at -20°C until immunohistochemical staining was performed. The sections were blocked in a blocking solution containing 5% normal donkey serum (Jackson Immunoresearch, Bar Harbor, ME, USA), 2% BSA (Sigma), and 0.1% Triton X-100 (Sigma) for 1 h at room temperature. The sections were then incubated with mouse anti-NeuN (1:1,000, Millipore, MAB377B), mouse GFAP (1:1,000, Millipore, MAB360), rabbit Iba1 (1:1,000, Wako, 019-19741), and rabbit c-Fos (1:1,000, Oncogene, PC05-100UG) antibodies overnight at 4°C in blocking solution. After washing with 0.1 M PBS containing 0.1% Triton X-100, the sections were incubated for 2 h with FITC-conjugated secondary antibodies (1:200, Jackson Immunoresearch, 715-095-151, 711-095-152) in blocking solution at room temperature, washed 3 times, and then mounted on gelatin-coated slide glass using Vectashield (Vector Laboratories, Inc. Burlingame, CA, USA). Fluorescent images of the mounted sections were obtained with a confocal microscope (LSM800, Carl Zeiss, Jena, Germany).

Electrophysiology

Transverse prefrontal cortical slices (300 μm) were prepared. Briefly, mice were

anesthetized with isoflurane and decapitated, and the brains were rapidly removed and placed in ice-cold, oxygenated (95% O_2 and 5% CO_2), low-Ca^{2+}/high-Mg^{2+} dissection buffer containing 5 mM KCl, 1.23 mM NaH_2PO_4, 26 mM $NaHCO_3$, 10 mM dextrose, 0.5 mM $CaCl_2$, 10 mM $MgCl_2$, and 212.7 mM sucrose. Slices were transferred to a holding chamber in an incubator containing oxygenated (95% O_2 and 5% CO_2) artificial cerebrospinal fluid (ACSF) composed of 124 mM NaCl, 5 mM KCl, 1.23 mM NaH_2PO_4, 26 mM $NaHCO_3$, 10 mM dextrose, 2.5 mM $CaCl_2$, and 1.5 mM $MgCl_2$ at 28-30°C for at least 1 h before recording. After recovery, slices were transferred to a recording chamber where they were perfused continuously with ACSF gassed with 95% O_2/5% CO_2 at a flow rate of 2 ml/min. Slices were equilibrated for 5 min prior to recordings, and all experiments were performed at 23-25°C. Recordings were obtained using a Multiclamp 700B amplifier (Molecular Devices, Sunnyvale, CA, USA) under visual control with differential interference contrast illumination on an upright microscope (BX51WI; Olympus, Tokyo, Japan). Patch pipettes (5–7 MΩ) were filled with 135 mM K-gluconate, 8 mM NaCl, 10 mM HEPES, 2 mM ATP-Na, and 0.2 mM GTP-Na to record sEPSCs and mEPSCs in the voltage-clamp (VC) mode or neuronal excitability in the current-clamp (CC) mode (pH 7.4 and 280-290 mOsm). Only cells with access resistance < 20 MΩ and input resistance >100 MΩ were studied. The extracellular recording solution consisted of ACSF supplemented with picrotoxin (100 μM) and tetrodotoxin (1 μM) for mEPSC experiment. Data were acquired and analyzed using pClamp 10.5 (Molecular Devices). Signals were filtered at 2 kHz and digitized at 10 kHz using Digidata 1550A (Axon Instruments, Union City, CA, USA).

Gliotransmitter assays

A concentration of glutamate, D-serine, and ATP were measured using ELISA kits according to the respective manufacturer's instructions (Glutamate Colorimetric Assay kit, Biovision, #K629-100; DL-serine Assay Kit, Biovision, #K743-100; ATP Assay System Bioluminescence Detection Kit, Sigma, #11 699 709 001). dmPFC tissue was collected from rank-1, rank-4, light stimulated rank-4-GFAP-mCherry and rank-4-GFAP-ChR2 mice, respectively. All tissues were homogenized and centrifuged for the assay. All assays were conducted using a 96-well microplate immediately after sample collection.

In vivo microdialysis with light stimulation

After surgery, a CMA7 microdialysis probe (shaft length 5 mm; shaft outer-diameter 0.58 mm) was implanted through the guide cannula. The probe was connected to a CMA100 microinjection pump (CMA Microdialysis) with polyethylene tubing (PE 50) and FEP tubing (INSTECH, Plymouth meeting, PA, USA). Then the probe was perfused with ACSF (in mM: 149 NaCl, 2.8 KCl, 1.2 MgCl2, 1.2 CaCl2, and 5.4 glucose, pH7.4) into the inlet of the probe at a flow rate of 1.5 μl/min. Perfusates from the outlet of the tubing were automatically collected in plastic vials at 8°C using a CMA 470 refrigerated fraction collector. Dialysates were collected over 30 min intervals for 3 h and used for measurement of glutamate from the second samples. Light was delivered for 5 min (473 nm, 20 Hz, 25 ms of pulse duration, 1 min inter-stimulus interval) at 1.5 h after the beginning of the experiment. Dialysates were stored at -80°C and then glutamate

concentration was analyzed.

Surface protein biotinylation and immunoblot analysis

dmPFC tissues were prepared from 8- to 12-week-old rank-1, rank-4, rank-4-GFAP-mCherry, and rank-4-GFAP-ChR2-mCherry mice using the same method of slice preparation as for electrophysiology and were sliced into 300 μm thickness. The mPFC slices were recovered for 30 min at 31°C in oxygenated ACSF. To biotinylate the surface proteins, the slices were incubated with 1mg/ml sulfo-NHS-SS-biotin (Thermo Scientific, 21328) in ACSF at 4°C for 45 min. The slices were quenched with 100 mM glycine in ACSF at 4°C for 25 min after washing with ACSF. The quenched slices were lysed with RIPA buffer (50 mM Tris, pH7.5, 0.1% SDS, 1% Triton X-100, 150 mM NaCl, 0.5 sodium deoxycholate and 2 mM EDTA) containing protease inhibitor cocktail (Sigma-Aldrich, 11836153001), and incubated at 4°C rotating for 30 min. The lysates were centrifuged at 15,000 g for 15 min at 4^{o}C and supernatant was collected. The concentration of protein was determined via BCA Protein Assay Kit (Thermo Scientific, 23225). To isolate biotinylated proteins, 200 μg of each sample was added to streptavidin-agarose beads (Thermo Scientific, 29200) and incubated at 4°C rotating overnight. The streptavidin-agarose beads were eluted with 2x laemmil sample buffer after washing with the lysis buffer and used for membrane surface proteins. Twenty μg of slice lysate was used for total proteins. The proteins were separated on SDS-PAGE gels and then transferred onto PVDF membranes. The membranes were blocked in 5% skim milk in TBS-T for 1 h at room temperature and incubated with primary antibodies in blocking buffer at 4°C overnight. Primary antibodies to

GluA1 (1:1,000, Millipore, MAB2263) and GluA2 (1:1,000, Millipore, MAB397) were applied. After washing, membranes were incubated with horseradish peroxidase (HRP)-conjugated secondary antibodies for 1 h at room temperature. HRP was detected using Super Signal West Femto Maximum Sensitivity Substrate (Thermo Scientific, 34096) and a Bio-Image Analyzer (MicroChemi/DNR, Neve Yamin, Israel).

Statistics

Statistical significance was determined using the two-tailed Student's *t*-test, paired *t*-test, Wilcoxon signed-rank test, or two-tailed Mann-Whitney *U*-test for comparison between two groups. For multiple comparisons, one-way ANOVA and Bonferroni's multiple comparison tests were used. All data are represented as the mean ± s.e.m., and differences were considered statistically significant when the *p*-value was less than 0.05.

Results

Optogenetic activation of dmPFC astrocytes induces winning by enhancing resistance behavior in the tube test

I assessed mice social hierarchy through the tube test, which is stable and correlates well with other dominance measures[120]. Four 6-week-old male mice were housed per cage for at least 2 weeks prior to the tube test. Mice were tested pair-wise, and social rank was assessed on the basis of the number of wins against the other three cage mates. Cages in which the mice maintained a stable hierarchy for at least 3 consecutive days were considered as social hierarchy-established cages and utilized for further investigations (Fig. 1a). In tube tests among the cage mates, winner mice pushed and resisted more against loser mice (Fig. 1b). The body weight of the test mice did not vary depending on their social hierarchy from 6 weeks to 13 weeks. However, after 14 weeks, body weight was divided into two groups (dominants vs. subordinates) (Fig. 1c and d). The percentage of hierarchy-established cages was consistent (62~68%) regardless of tube test time of day (Fig. 1e) or age of the mice tested (Fig. 1f), validating test consistency.

dmPFC astrocyte activation while MDT-dmPFC neural circuit activation further potentiates and maintains rank elevation of rank-4 mice.

To investigate astrocyte function in behaving mice *in vivo*, I employed both chemogenetic and optogenetic techniques that enabled astrocyte activity manipulation. I simultaneously delivered AAVDJ-CamKII-ChR2-eGFP into right MDT and AAV5-gfaABC1D-hM3Dq-mCherry into right PL region of rank 4 mice

(Fig. 2a-c). After 2 weeks, I chemogenetically activated dmPFC astrocytes by introducing CNO (i.p., 3 mg/kg) while optogenetically activating MDT to dmPFC neural circuit. As previously reported[14], optogenetic MDT-dmPFC circuit stimulation elevated social hierarchy of rank 4 mice (Fig. 2d gray). When we activated dmPFC astrocytes along with optogenetic MDT-dmPFC circuit stimulation, it further potentiated and maintained the elevated ranks of rank 4 mice (Fig. 2d yellow).

Chemogenetic dmPFC astrocyte stimulation induces rank elevation of rank-4 mice.

Considering that simultaneous activation of neuron and astrocyte can maintain hierarchical rank elevation, I next tested whether astrocyte alone can trigger rank change in rank-4 mice. To confirm if astrocyte activation per sei controls social rank, we infected AAV5-gfaABC1D-hM3Dq-mCherry into PL region and performed tube test with CNO injection (i.p., 3 mg/kg) (Fig. 3a). CNO-injected rank 4 mice showed significant rank elevation at 2 and 6 h after CNO injection (Fig. 3b). Interestingly, chemogenetic astrocyte activation increased mouse resistance behavior but not pushing behavior during fight (Fig. 3c). To examine the effect of chemogenetic dmPFC astrocyte stimulation on synaptic input into dmPFC, I performed miniature excitatory post-synaptic current (mEPSC) of PL layer V pyramidal neurons using acute brain slices. The result showed significant increases in mEPSC frequency, but not mEPSC amplictude, in PL Layer V pyramidal neurons upon chemogenetic astrocyte stimulation (Fig. 3d).

Optogenetic dmPFC astrocyte stimulation increases extracellular Ca^{2+}.

Next, I employed optogenetic techniques that enabled astrocyte activity manipulation with temporal precision to investigate astrocyte function in behaving mice *in vivo*. Optogenetic activation of ChR2-expressing astrocytes has been shown to trigger an intracellular calcium increase in prior study[125], as was confirmed in my study *in vitro* (Fig. 4a-c). Next, AAVDJ expressing ChR2 under the control of the astrocytic glial fibrillary acidic protein (GFAP) promotor (AAVDJ-GFAP-ChR2-mCherry) or control virus (AAVDJ-GFAP-mCherry) was injected into the right PL subregion of the dmPFC (Fig. 4d). Within the virally transduced region, ChR2 expression was limited to astrocytes with high specificity (> 97% of GFAP positive cells) (Fig. 4e). Co-staining with neuronal nuclei (NeuN) and microglial marker Iba1 showed negligible overlaps (0.8% and 1.6%, respectively) (Fig. 4e).

Optogenetic dmPFC astrocyte stimulation induces rank graduation of rank-4 mice by increasing their resistance behavior.

Upon implanting an optic fiber 3 weeks after the viral injection, I delivered a 473-nm laser stimulation at 20-Hz (25 ms of pulse duration), a protocol that has been used to stimulate astrocytes[125], to rank-4 mice 30 seconds prior to the tube test, and kept the light on throughout the test until the tube test was over maximum for two minutes. Upon light stimulation, the rank of AAVDJ-GFAP-ChR2-mCherry-injected mice (GFAP-ChR2 mice), but not AAVDJ-GFAP-mCherry-injected mice (GFAP-mCherry mice), was elevated significantly (Fig. 5a and b). Interestingly, optogenetic astrocyte stimulation increased resistance

behavior rather than pushing behavior during the fight (Fig. 5c and d), which was sufficient for rank graduation. There were no correlations between virus transduction area and rank change rate or time (Fig. 5e). Moreover, optogenetic astrocyte stimulation induced a rank change in around 80% of mice regardless of experimental conditions (light, dark or random phase) (Fig. 5f). In conclusion, dmPFC astrocyte activation induces dominance behavior by enhancing resistance against opponents during fights in the tube test.

Optogenetic astrocyte stimulation influences excitatory synaptic input to pyramidal neurons, but not their excitability

I next investigated the effect of astrocyte activation on the neuronal activity of layer V pyramidal neurons in the dmPFC. To examine the effect of optogenetic dmPFC astrocyte stimulation on synaptic release including miniature excitatory post-synaptic current (mEPSC) and spontaneous EPSC (sEPSC), I performed whole-cell recordings of dmPFC pyramidal neurons in this region in acute brain slice. In GFAP-ChR2 mice, the frequency of both mEPSCs and sEPSCs was significantly elevated not only during light stimulation but also when the light was turned off up to 2 min (Fig. 6a-c). Meanwhile, the amplitudes of mEPSCs and sEPSCs were not altered (Fig. 6c and d), and neither neuronal excitability nor the action potential threshold was affected by astrocyte activation (Fig. 7). These observations show that dmPFC astrocytic activation induced prolonged increases in the frequency of synaptic inputs, without altering the amplitude of synaptic currents and excitability.

Optogenetic dmPFC astrocyte stimulation does not alter basal aggressive behavior.

I further investigated that whether dmPFC astrocyte stimulation affects basal aggressive behavior of mice. I performed resident-intruder (RI) test to investigate mouse aggressive behavior (Fig. 8a). Male C57BL/6J mice divided by two groups showing non-aggressive or aggressive behaviors (Fig. 8b). Then I optogenetically stimulated dmPFC astrocyte of resident mice whether they alter aggressiveness. Optogenetic dmPFC astrocyte stimulation did not affect basal aggressiveness in both non-aggressive (Fig. 8c) and aggressive mice (Fig. 8d). In conclusion, dmPFC astrocyte activation does not alter aggressiveness of mice.

Optogenetic dmPFC astrocyte stimulation does not alter locomotion, anxiety, and depressive behaviors.

I also investigated that whether dmPFC astrocyte stimulation affects mouse locomotion and mood behaviors such as anxiety and depression. I performed OFT to investigate locomotive behavior, and EPM and FST to investigate mouse anxiety and depressive behaviors along with optogenetic dmPFC astrocyte stimulation. Optogenetic dmPFC astrocyte stimulation did not affect basal locomotion such as total distance traveled (Fig. 9a and b). Distance in center in OFT (Fig. 9c-e) and time in open arm in EPM (Fig. 9f and g) suggest that anxiety-like behavior did not altered by optogenetic dmPFC astrocyte stimulation. Furthermore, according to the result of time immobility in FST indicate that depressive-like behaviors did not altered by dmPFC astrocyte activation (Fig. 9h). In conclusion, dmPFC astrocyte activation does not alter mood behaviors such as

anxiety and depression of mice. In conclusion, dmPFC astrocyte activation was sufficient to induce dominance behavior by enhancing resistance against opponents during fights in the tube test without affecting aggressiveness or mood.

Optogenetic dmPFC astrocyte stimulation induces extracellular glutamate release.

Next, I investigated putative gliotransmitters released from the astrocytes after light stimulation. Thus far three types of gliotransmitters have been reported as derived from activated astrocytes; D-serine, ATP, and glutamate[126]. In dmPFC tissue, only glutamate, and not D-serine, DL-serine, or ATP, was increased after optogenetic astrocyte stimulation (Fig. 10a). I also verified an increase in extracellular glutamate level in the dmPFC after astrocyte stimulation *in vivo* using microdialysis; dmPFC extracellular glutamate level increased right after optogenetic astrocyte stimulation *in vivo* (20-Hz, 25 ms, 5 min with 1 min interval), which lasted up to 1 h (Fig. 10b).

Surface AMPA receptor expression is increased after optogenetc dmPFC astrocyte stimulation.

I expected the glutamate receptor-mediated synaptic current to be influenced by astrocyte-derived glutamate, and therefore conducted whole-cell patch clamp experiments to measure AMPA receptor-mediated synaptic current, as well as mEPSCs in the dmPFC slices of rank-1, rank-4, and light-stimulated rank-4 mice. I found significantly lower mEPSC amplitudes in basal rank-4 mice compared to rank-1 mice (Fig. 11a). Of note, rank-4 mice who had raised their rank

upon optogenetic astrocyte stimulation exhibited elevated mEPSC amplitudes comparable to rank-1 mice without astrocyte stimulation (Fig. 11a). These results suggest that increased extracellular glutamate level by astrocyte stimulation elevated AMPA receptor-mediated synaptic input into dmPFC pyramidal neurons in rank-4 mice.

To investigate the molecular mechanisms underlying the correlation between dominance behavior and the amplitude of mEPSC current in dmPFC neurons, I measured membrane expression levels of GluA1 and GluA2, two major subunits of the AMPA receptor, in the dmPFC. Membrane GluA1 expression level in rank-4 mice was lower than in rank-1 mice, and was significantly increased by astrocyte stimulation (Fig. 11b). This change indicated that membrane GluA1 levels correlate with social hierarchy. Meanwhile, membrane GluA2 expression level did not correlate with mice social hierarchy (Fig. 11b).

AMPA receptor antagonist, NBQX, successfully block dmPFC astrocyte induced rank graduation.

I next tested if AMPA receptor function directly influenced dominance behavior. I implanted both a guide cannula and optic fiber in the PL subregion of the dmPFC to simultaneously block the AMPA receptor and stimulate astrocytes. I injected NBQX, an AMPA receptor antagonist, or vehicle to the PL area of rank-4 mice in their home cage 30 min prior to the tube test (Fig. 12a). NBQX infusion almost completely abrogated the rank changes due to astrocyte stimulation (Fig. 12b). NBQX treatment did not affect motor activity or mood, which were measured by the open field test, elevated plus maze, and force swim test (Fig. 13). Taken

together, these data support that glutamate released from astrocytes regulates AMPA receptor-mediated synaptic inputs to pyramidal neurons in the dmPFC and thereby modulates dominance competition.

Astrocyte stimulation induces dominancy as effectively as pyramidal neuron stimulation but with distinct behavioral strategy

Since dmPFC pyramidal neurons regulate dominance behavior as well[13,14], I next compared astrocyte stimulation-induced dominance behavior with the results of pyramidal neuron stimulation. Mice were divided into two groups: one with neuronal ChR2 expression by AAVDJ-hSyn1-ChR2-mCherry injection (hSyn1-ChR2 mice) and another with astrocytic ChR2 expression by AAVDJ-GFAP-ChR2-mCherry injection (GFAP-ChR2 mice) in the dmPFC area. Upon light stimulation during the tube test (473 nm, 20 Hz, 25 ms), the average rank change of rank-4 mice was comparable between these two groups (Fig. 14a and b). As previously reported, neuronal stimulation induced rank change by increasing both pushing and resisting behaviors (Fig. 14a)[14]. However, GFAP-ChR2 mice did not exhibit elevated pushing behavior, although the level of rank induction was similar to those of hSyn1-ChR2 mice (Fig. 14a). Next, I measured the winning rate of each group competing with their matched control (AAV-hSyn1-mCherry-injected mice and AAVDJ-GFAP-mCherry-injected mice, respectively) (Fig. 14b). Both groups showed comparable winning rates in the tube test against control mice (~75%) (Fig. 14b). I then arranged matches between hSyn1-ChR2 mice and GFAP-ChR2 mice with light stimulation (473-nm, 20-Hz, 25 ms) (Fig. 14c). Since neuronal ChR2 stimulation increased pushing behavior while astrocyte stimulation did not, I

expected hSyn1-ChR2 mice to dominate over GFAP-ChR2 mice. However, the winning rate between the two groups was not different; the winning rate of neuronal ChR2-stimulated mice was 53.8% and that of astrocyte ChR2-stimulated mice was 46.2% (Fig. 14c). These data indicate that an increase in resistance *via* astrocyte stimulation contributed to mouse dominancy as much as an increase in pushing behavior *via* neuronal stimulation. Taken together, both neurons and astrocytes in the dmPFC equally contribute to mouse dominance behavior, however, their activation employs distinct behavioral strategy to achieve dominancy during social competition (Fig. 15).

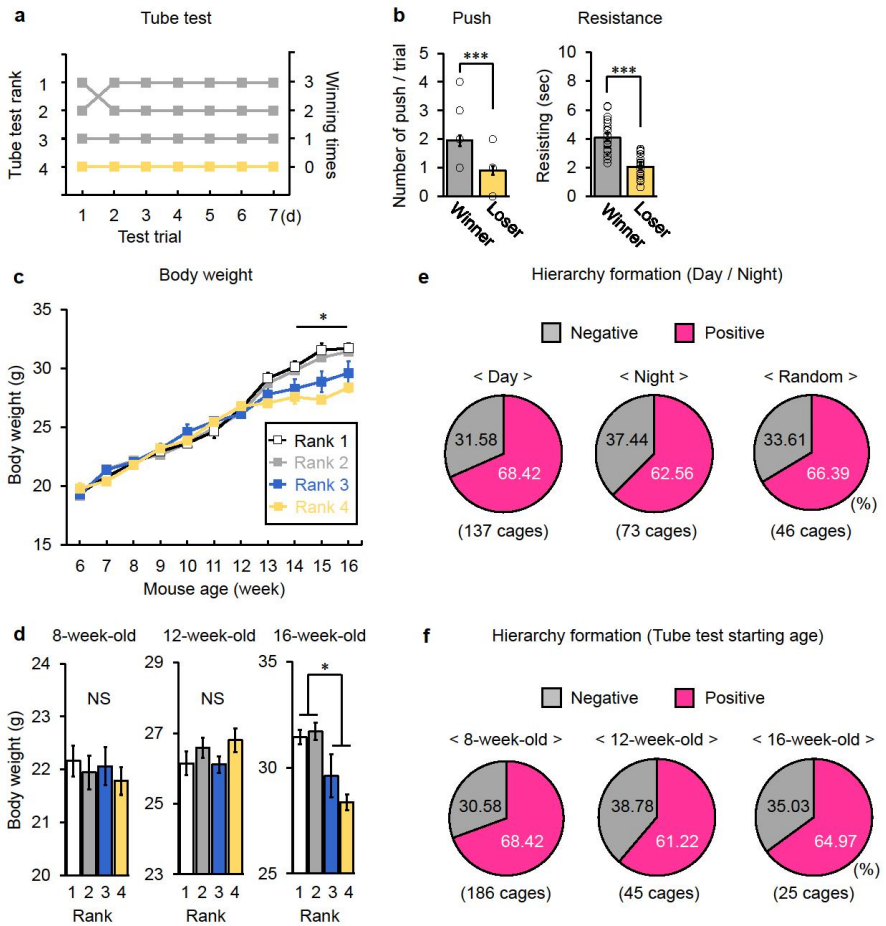

Figure 1. Formation of social hierarchy in the group-housed mice. a, Basal hierarchy by performing daily tube test of a mouse cage. **b**, The number of pushing and resistance behaviors per tube test trial of winner mice compared to losers (n=22 in each group). Two tailed t-test. **c**, Body weights of all cage mates (from rank-1 to rank-4 mice) measured every week from 6- to 16-week-old (n=17 in each group). The body weight of the test mice did not vary depending on their social hierarchy from 6 weeks to 13 weeks. However, after 14 weeks, body weight was divided into two groups (dominants vs. subordinates). **d**, Body weights of all cage mates at ages 8-, 12-, and 16-week-old. One-way ANOVA, Bonferroni post-hoc analysis. **e** and **f**, The percentage of hierarchy formation according to tube test schedules (experiments conducted in light, dark, and random phases), and mouse ages. The percentage of hierarchy-established cages was consistent regardless of tube test time of day (62~68%) or age of the mice tested (61~68%) validating test consistency. *p < 0.05; ***p < 0.001; NS, not significant. Data are presented as the mean ± s.e.m.

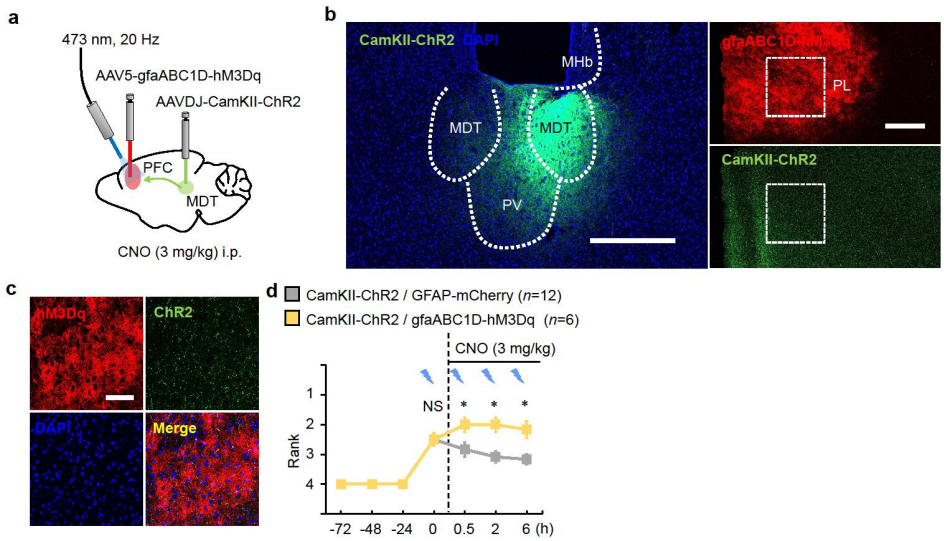

Figure 2. Simultaneous activation of MDT-dmPFC neural circuit and dmPFC astrocytes elevates and maintains rank graduation. a, Schematic illustration of virus injection of AAV5-gfaABC1D-hM3Dq-mCherry into dmPFC and AAVDJ-CamKII-ChR2-eGFP into MDT region, and simultaneous activation of dmPFC astrocytes and MDT-dmPFC neural circuit. **b,** Virus expression in the MDT and dmPFC region. Scale bar, (*Left*) 500 μm and (*Middle*) 1 mm. **c**, Astrocytes (hM3Dq-mCherry) in the PL subregion of dmPFC. eGFP fluorescence in the synaptic terminal of MDT neurons can be detected in this region. Scale bar, 100 μm. **d**, Optogenetic MDT-dmPFC circuit stimulation elevates hierarchical rank of rank-4 mice (gray). Chemogenetic activation of dmPFC astrocytes (i.p. injection of CNO (3 mg/kg)) along with optogenetic MDT-dmPFC circuit stimulation potentiated and maintained the elevated ranks of rank-4 mice (red). *p < 0.05; NS, not significant. Data are presented as the mean ± s.e.m.

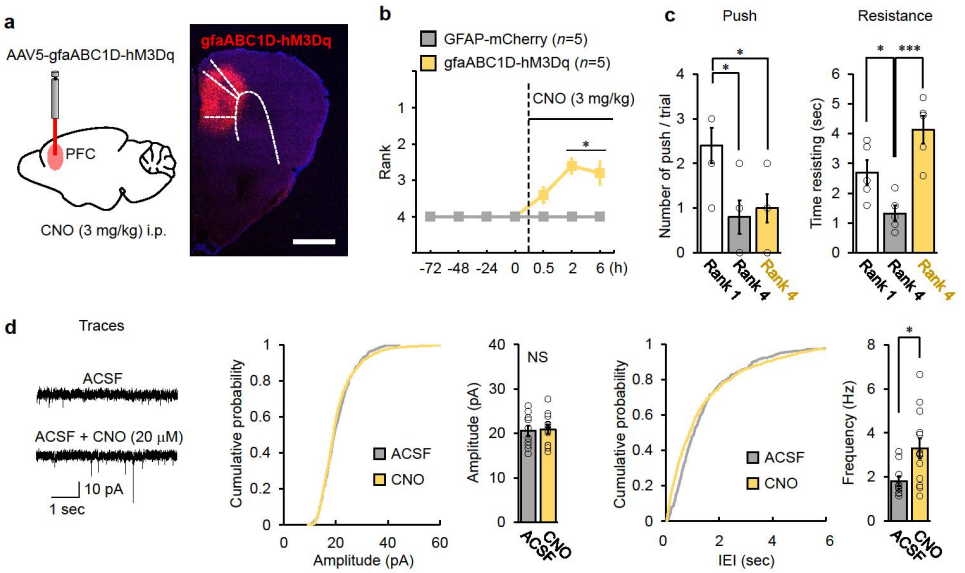

Figure 3. Chemogenetic activation of astrocyte in dmPFC increases hierarchical rank elevation of rank-4 mice by enhancing resistance behavior, and increases excitatory synaptic input into layer V pyramidal neuron. a, Expression of AAV5-gfaABC1D-hM3Dq-mCherry in the prelimbic cortex of dmPFC. Scale bar, 1 mm. **b,** Mean rank change of chemogenetic astrocyte-stimulated rank-4 mice injected with AAV5-gfaABC1D-hM3Dq-mCherry virus compared to their control group (AAVDJ-GFAP-mCherry) (*n*=5 in each group). Wilcoxon signed-rank test. **c**, Comparison of behavioral performances such as pushing and resistance of rank-1 and rank-4 mice during the tube competition (*n*=5 in each group). One-way ANOVA, Bonferroni post-hoc analysis. **d**, (*Left*) Representative traces of mEPSC events, and (*Middle and Right*) amplitude and frequency of mEPSC (10 cells from 3 GFAP-mCherry mice and 13 cells from 3 gfaABC1D-hM3Dq mice). Paired *t*-test. *p < 0.05; ***p < 0.001; NS, not significant. Data are presented as the mean ± s.e.m.

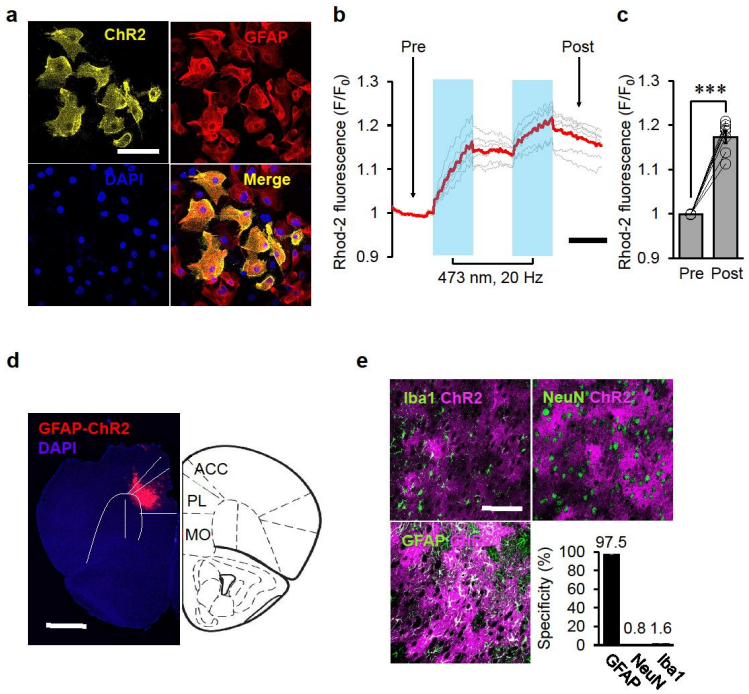

Figure 4. Optogenetic astrocyte stimulation increases intracellular Ca^{2+} response *in vitro*, and astrocyte-specific expression of ChR2 in dmPFC region *in vivo*. **a**, Fluorescence images of ChR2 (EYFP), astrocytes (GFAP), and both merged in cultured primary astrocytes. Scale bar, 100 μm. **b**, Ca^{2+} response in primary astrocytes *in vitro*. Rhod-2 fluorescence from individual astrocytes (gray) and averaged trace (red) in ChR2-positive astrocytes (7 cells). Optogenetic stimulation of ChR2-expressing astrocytes triggered an intracellular calcium increase. Scale bar, 1 min. **c**, Ca^{2+} responses of 'pre' and 'post' light stimulation of astrocytes. (Both 'pre' and 'post' are corresponded to the arrows in **b**). Two-tailed Mann-Whitney *U*-test. **d**, AAVDJ-GFAP-ChR2-mCherry was injected into the PL subregion of the dmPFC. Scale bar, 1 mm. **e**, mCherry signals (ChR2-positive cells) are expressed in astrocytes with more than 97% specificity. Negligible co-localization of ChR2 (mCherry) with the neuronal nuclear marker NeuN (0.8%) or the microglia marker Iba1 (1.6%) was detected. Scale bar, 100 μm. ***$p<0.001$. Data are presented as the mean ± s.e.m.

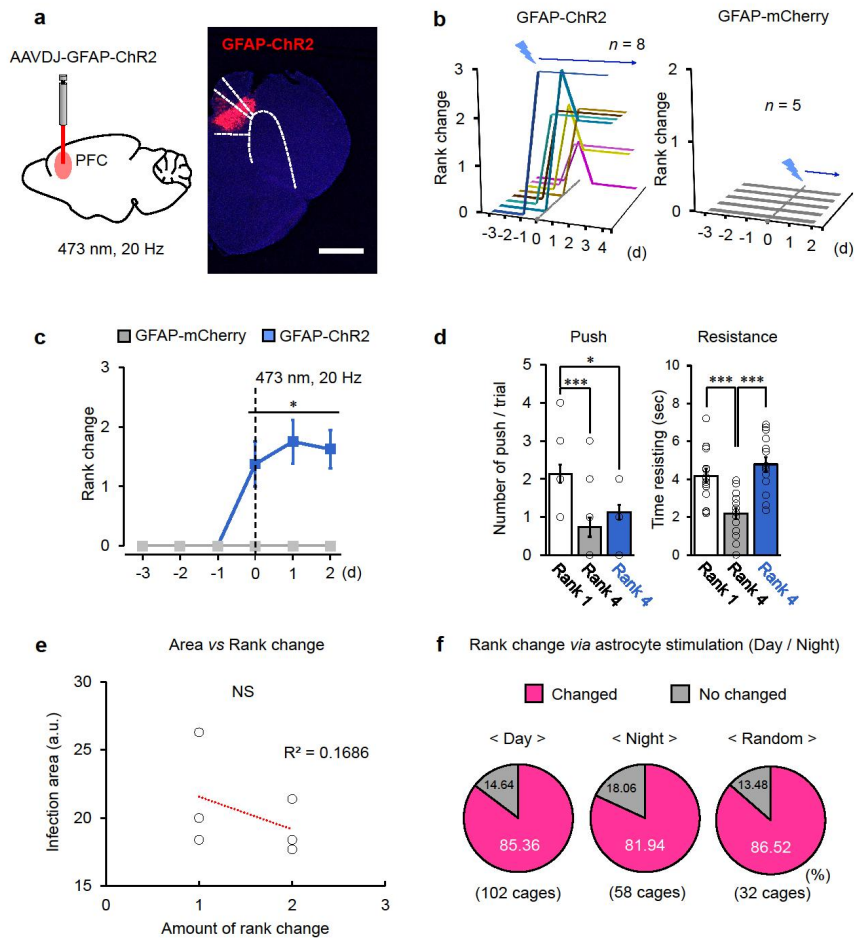

Figure 5. Optogenetic activation of dmPFC astrocytes induces winning by enhancing resistance behavior. a, GFAP-ChR2 virus expression in the dmPFC region. **b**, Individual rank change of dmPFC astrocyte-stimulated rank-4 mice injected with (*Left*) AAVDJ-GFAP-ChR2-mCherry (*n*=8) and (*Right*) AAVDJ-GFAP-mCherry (*n*=5) (20-Hz). **c**, Mean rank change of astrocyte-stimulated rank-4 mice injected with AAVDJ-GFAP-ChR2-mCherry virus compared to their control group (GFAP-mCherry) (*n*=5 for GFAP-mCherry and *n*=8 for GFAP-ChR2). Wilcoxon signed-rank test. **d**, Comparison of behavioral performances such as pushing and resistance of rank-1 and rank-4 mice during the tube competition (*n*=13 for rank-1 and rank-4 mice, and *n*=17 for AAVDJ-GFAP-ChR2-injected rank-4 mice with light stimulation (blue bars)). One-way ANOVA, Bonferroni post-hoc analysis **e**, Correlation between the virus infected area in the PL subregion of the dmPFC and rank changes. Pearson's correlation. **f**, The probability of rank change of rank-4 mice *via* optogenetic dmPFC astrocyte stimulation (tube tests were conducted in light, dark, and random phases). Optogenetic astrocyte

stimulation induced a rank change in around 80% of mice regardless of experimental conditions (light, dark or random phase) *p<0.05; ***p<0.001; NS, not significant. Data are presented as the mean ± s.e.m.

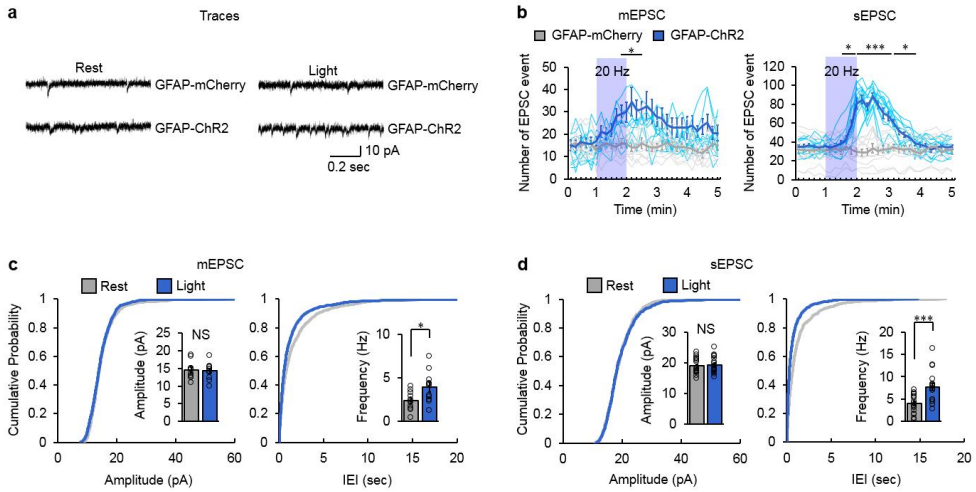

Figure 6. Optogenetic activation of dmPFC astrocytes elicits a synaptic input increase. a, Representative traces of mEPSC events. **b**, Number of mESPC (*Left*) and sEPSC (*Right*) events per 10 sec time bin, before, during and after astrocyte stimulation (1 min of 20-Hz) (mEPSC: 10 cells from 3 GFAP-mCherry mice and 11 cells from 3 GFAP-ChR2 mice; sEPSC: 23 cells from 5 GFAP-mCherry mice and 17 cells from 4 GFAP-ChR2 mice). Wilcoxon signed-rank test. **c** and **d**, Cumulative probabilities and mean results of both amplitude and frequency of mEPSC (c) and sEPSC (d) (mEPSC: 10 cells from 3 GFAP-ChR2 mice; sEPSC: 17 cells from 4 GFAP-ChR2 mice). EPSC frequency, not amplitude, increase was observed in both mEPSC and sEPSC upon light stimulation. Two-tailed Mann-Whitney *U*-test. *p<0.05; ***p<0.001; NS, not significant. Data are presented as the mean ± s.e.m.

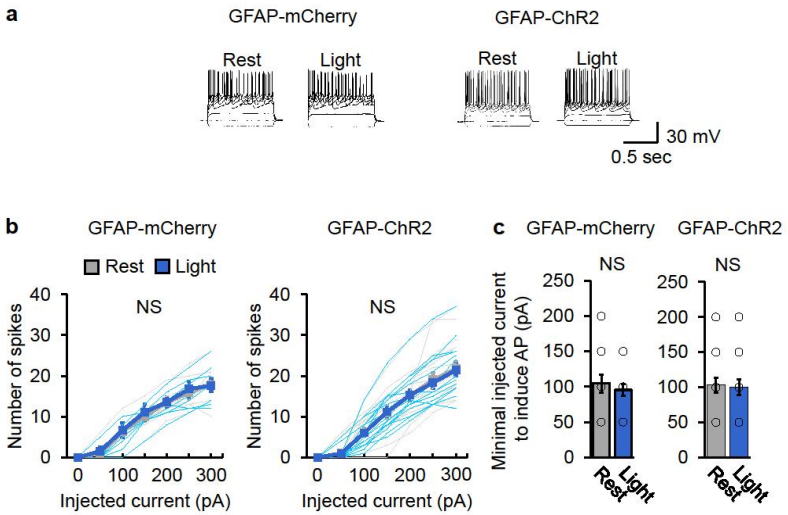

Figure 7. Optogenetic activation of dmPFC astrocytes does not affect neuronal excitability. a, Representative traces of excitability of GFAP-mCherry and GFAP-ChR2. **b** Number of action potentials at different current steps of GFAP-mCherry (9 cells from 3 mice) and GFAP-ChR2 (17 cells from 4 mice). Paired *t*-test. **c**, The minimal injected current to induce action potential from resting and light-stimulated pyramidal neurons of GFAP-mCherry and GFAP-ChR2; Paired *t*-test. NS, not significant. Data are presented as the mean ± s.e.m.

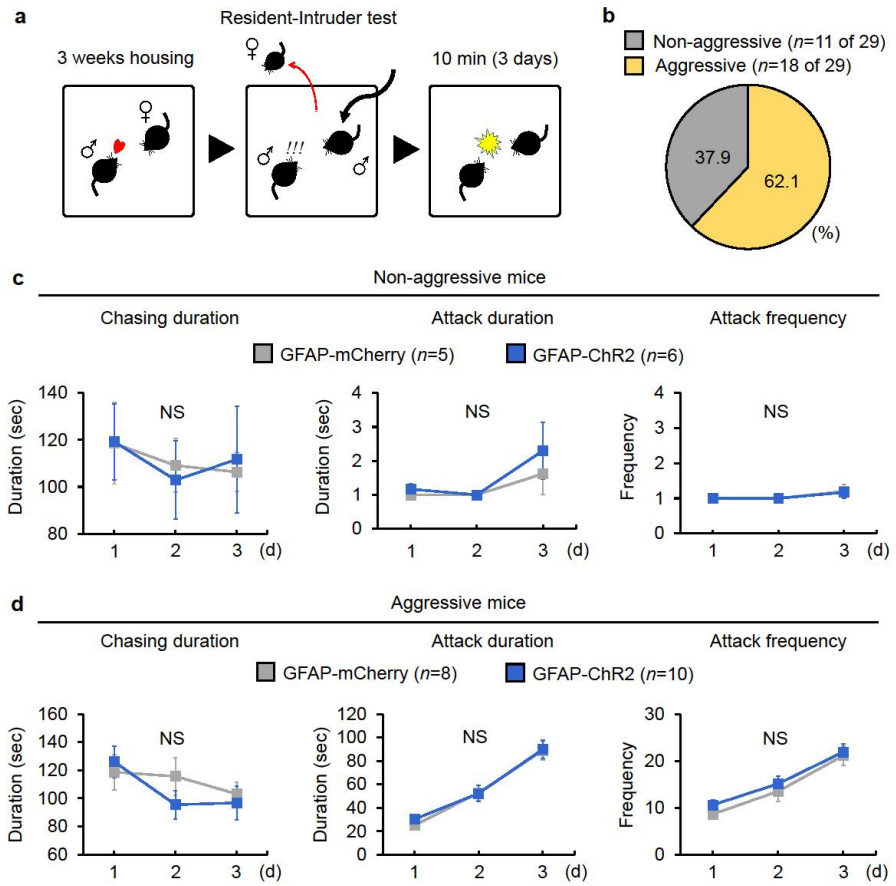

Figure 8. Aggressive behaviors are not affected by optogenetic dmPFC astrocyte stimulation. a, Schematic illustration of the resident-intruder test. Both male and female mice were housed together for 3-4 weeks. On the day of the test, the female mouse was removed and a new male mouse was introduced into the cage as an intruder. The behavior test was conducted for 10 min with light stimulation (473-nm, 20-Hz) during the experimental period (3 days). The behaviors were videotaped, and aggressive behaviors of resident mice were measured by counting their (*i*) chasing duration, (*ii*) attack duration, and (*iii*) attack frequency for 3 consecutive experimental days. **b**, Diagram of resident-intruder test results divided by aggressive (62.1 %) and non-aggressive resident mice (37.9 %). **c** and **d**, Mean results of chasing, attack duration, and attack frequency of (*Top row*) non-aggressive resident mice and (*Bottom row*) aggressive resident mice with light stimulation. Both attack duration and frequency increased daily in aggressive resident mice with repeated exposure to an intruder, however, the differences between the two groups (GFAP-mCherry vs. GFAP-ChR2) were not significant. Two-tailed Student's *t*-test. NS, not significant. Data are presented as the mean ± s.e.m.

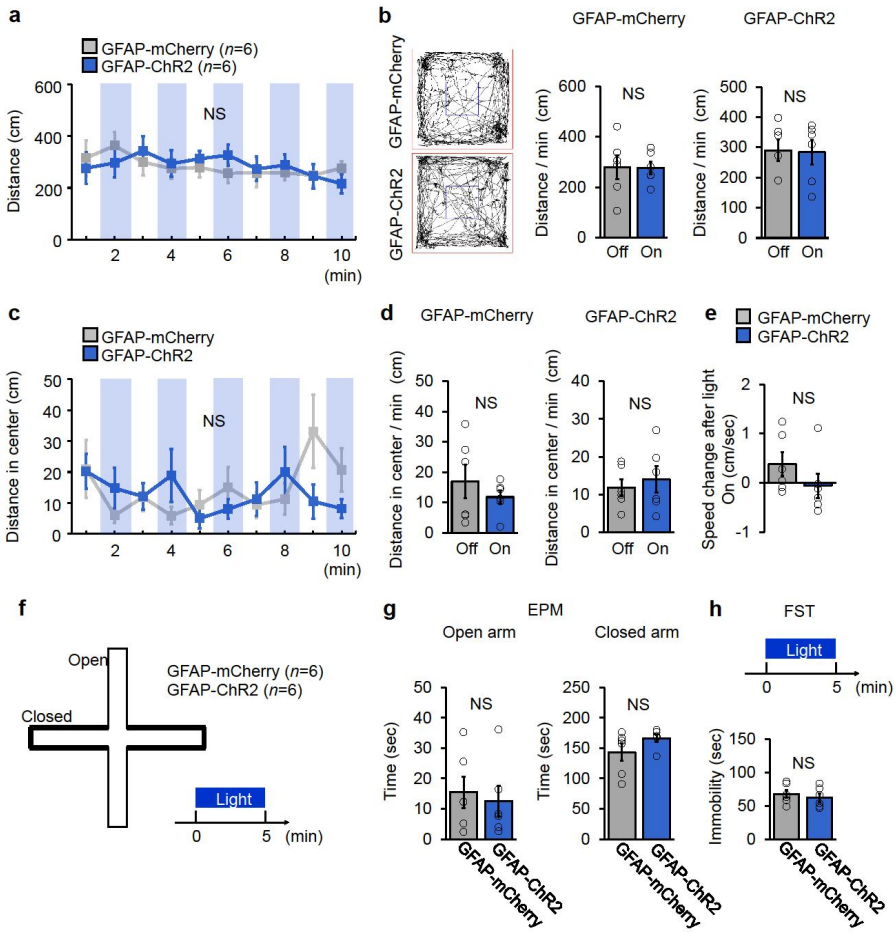

Figure 9. Optogenetic dmPFC astrocyte activation in the dmPFC region does not alter locomotion, anxiety, or depressive-like behavior. a, A result of mouse locomotion from OFT with intermittent light stimulation during a 10 min experimental period. **b**, (*Left*) Representative traces of mouse locomotion for 10 min and (*Middle* and *Right*) total distance traveled per 1 min with light on and off. **c**, Distance in center area with intermittent light stimulation during the 10 min experimental period. **d**, Distance traveled in the center per 1 min with light on and off during the test session. **e**, Difference in locomotion speed before and after the light stimulation. **f**, Schematic illustration of EPM with light stimulation. Light was delivered during experimental session (5 min) to test mice. **g**, Anxiety-like behaviors assessed by time spent in open and closed arms. **h**, Depressive-like behavior measured by immobility time in the FST (n=6 in each group). Light was delivered during experimental session (5 min) to test mice. Two-tailed Student's t-test. NS, not significant. Data are presented as the mean ± s.e.m.

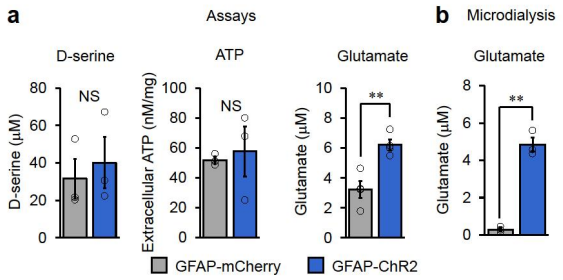

Figure 10. dmPFC astrocyte stimulation induces glutamate release. a, D-serine, ATP, and glutamate concentration in dmPFC slice via optogenetic stimulation of astrocytes in the dmPFC. (*n*=3 in each group). **b**, Extracellular glutamate concentration by *in vivo* microdialysis via optogenetic stimulation of astrocytes in the dmPFC (*n*=3 in each group). Paired *t*-test. **p < 0.01; NS, not significant. Data are presented as the mean ± s.e.m.

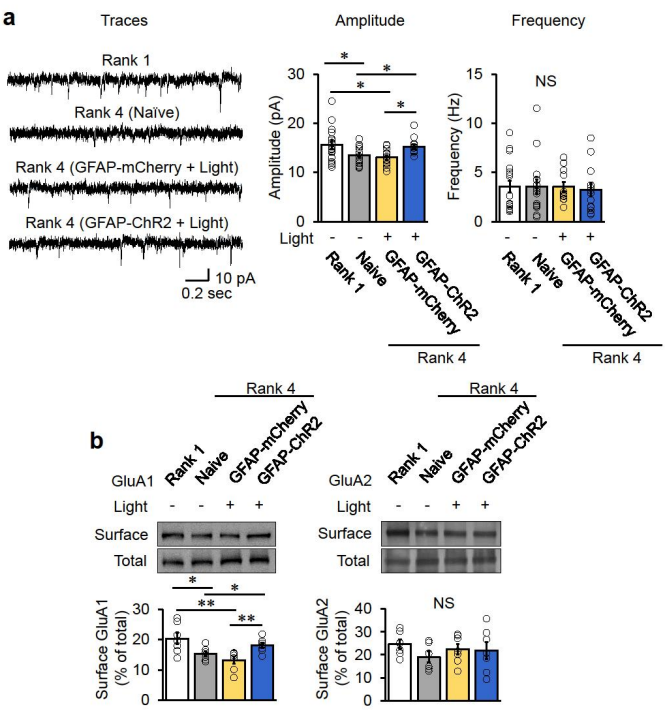

Figure 11. Optogenetic stimulation of dmPFC astrocyte modulates social hierarchy through AMPA receptor activation. a, (*Left*) Representative mEPSC traces from dmPFC layer V pyramidal neurons. (*Middle* and *Right*) Average mEPSC amplitude and frequency results after tube test with optogenetic stimulation of rank-4 mice (18 cells from 3 rank-1 mice, 15 cells from 3 rank-4 mice, 11 cells from 3 AAVDJ-GFAP-mCherry-injected rank-4 mice, and 13 cells from 3 AAVDJ-GFAP-ChR2-mCherry-injected rank-4 mice). One-way ANOVA, Bonferroni post-hoc analysis. **b**, Biotinylation assays of surface GluA1 and GluA2 from dmPFC tissue and averaged results (n=7 for rank-1, AAVDJ-GFAP-mCherry-injected rank-4, and AAVDJ-GFAP-ChR2-mCherry-injected rank-4 mice, and n=6 for rank-4 mice). One-way ANOVA, Bonferroni post-hoc analysis. *$p < 0.05$ and **$p < 0.01$ compared to rank-1; $^{\#}p<0.05$ and $^{\#\#}p<0.01$ compared to rank-4 of GFAP-ChR2. NS, not significant. Data are presented as the mean ± s.e.m.

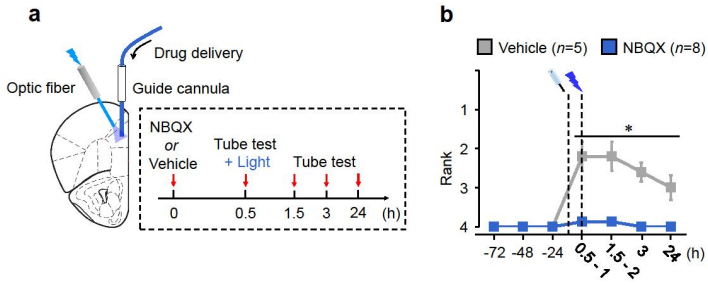

Figure 12. AMPA receptor antagonist, NBQX, does not induce hierarchical rank elevation of rank-4 mice. a, Schematic illustration of simultaneous implantation of both optic fiber and guide cannula in the PL region of the dmPFC. Experimental paradigm of NBQX or vehicle treatment 30 min before the tube test with or without light stimulation, as outlined by dashed line. **b**, The result of hierarchical rank changes by astrocyte stimulation following treatment with NBQX (blue, *n*=8) or vehicle (black, *n*=5) 30 min before light stimulation to rank-4 mice. Wilcoxon signed-rank test. *p < 0.05; NS, not significant. Data are presented as the mean ± s.e.m.

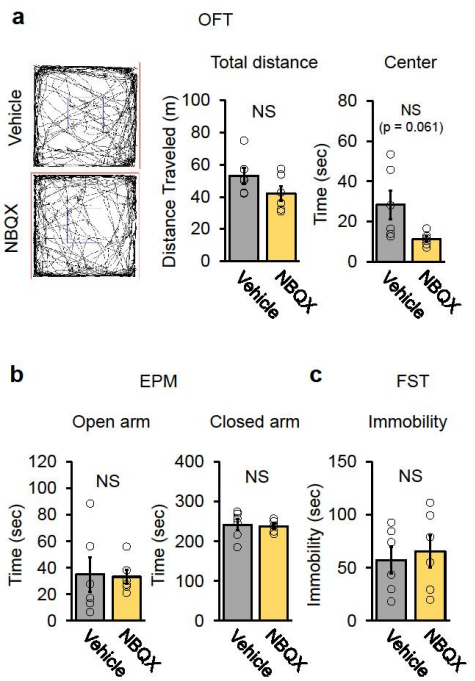

Figure 13. NBQX pretreatment in the dmPFC region does not alter locomotion, anxiety, or depressive-like behavior. **a**, A result of mouse locomotion from OFT (10 min). (*Left*) Representative traces of mouse locomotion, (*Middle*) total distance traveled, (*Right*) time in center area during the test session (5 min). **b**, Anxiety-like behaviors assessed by time spent in (*Left*) open and (*Right*) closed arms by EPM. **c**, Depressive-like behavior was measured by time immobility in the FST. All behavioral tests in were performed 30 min after treatment with vehicle or NBQX (n=6 in each group). Two-tailed Student's t-test. NS, not significant. Data are presented as the mean ± s.e.m.

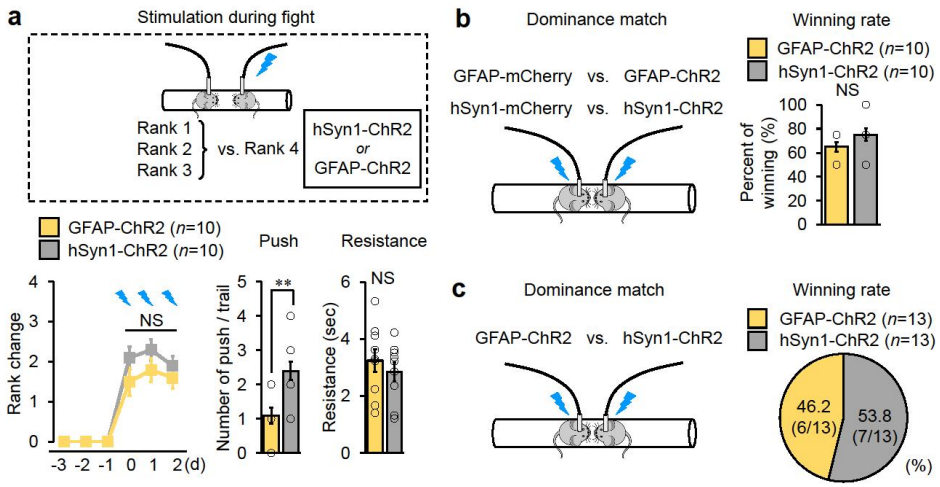

Figure. 14. Astrocytes and neurons in dmPFC employ distinct behavioral strategies to achieve dominancy during tube test. a, Schematic illustrations of the tube test procedures. Mice were divided into two groups: one with neuronal ChR2 expression by AAVDJ-hSyn1-ChR2-mCherry injection (hSyn1-ChR2 mice) and another with astrocytic ChR2 expression by AAVDJ-GFAP-ChR2-mCherry injection (GFAP-ChR2 mice) in the dmPFC area. Upon light stimulation during the tube test, the average rank change of rank-4 mice was comparable between these two groups. GFAP-ChR2 mice did not exhibit elevated pushing behavior, although the level of rank induction was similar to those of hSyn1-ChR2 mice. Wilcoxon signed-rank test and Student's two-tailed *t*-test. **b**, Schematic illustration of dominance competition between light-induced ChR2 injected mice (n=10 for GFAP-ChR2 and hSyn1-ChR2) and their matched control mice (n=10 for GFAP-mCherry and hSyn1-mCherry). Both groups showed comparable winning rates in the tube test against control mice. Student's two-tailed *t*-test. **c**, Schematic illustration of dominance competition between light-stimulated GFAP-ChR2 and hSyn1-ChR2 mice (n=13 in each group). The winning rate between the two groups was not different; the winning rate of neuronal ChR2-stimulated mice was 53.8% and that of astrocyte ChR2-stimulated mice was 46.2%. **p < 0.01; NS, not significant. Data are presented as the mean ± s.e.m.

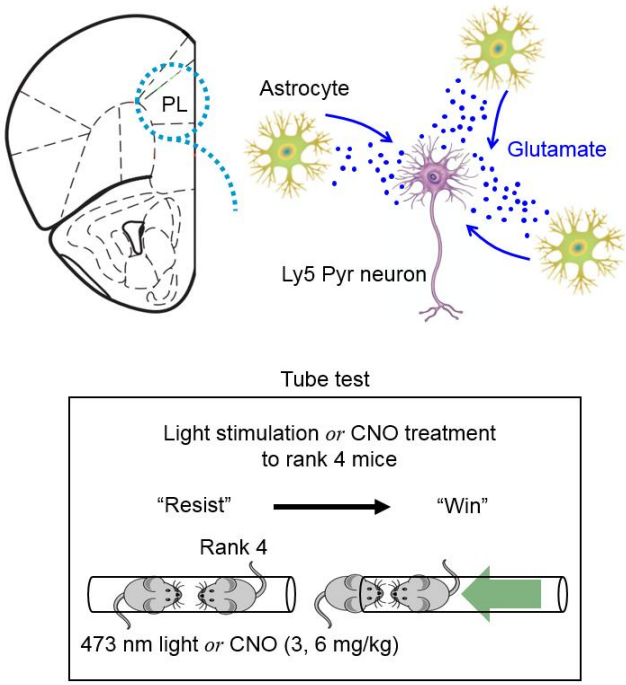

Figure 15. Graphical summary of the study. dmPFC astrocyte activation increases extracellular glutamate, and dmPFC layer V pyramidal neurons receive glutamatergic excitatory synaptic inputs. This induces mouse resistance behavior during social fight, and results in winning.

Discussion

These results demonstrate that optogenetic activation of dmPFC astrocytes induces winning in social competition and its maintenance via increasing resistance behavior. As an underlying mechanism, I discovered that astrocyte activation induced prolonged enhancement of excitatory synaptic inputs to dmPFC layer V pyramidal neurons without affecting excitability. Therefore, I propose that such synaptic potentiation by astrocyte activation induces long-term winning during social competition (Fig. 15).

Of note, my data show that astrocytes play a distinct role in social dominance behavior compared to neurons. Optogenetic astrocyte stimulation elevated mouse social hierarchy in tube tests via a different behavioral strategy compared to neuronal stimulation. Optogenetic stimulation of dmPFC pyramidal neurons elevated mouse social hierarchy by increasing both pushing and resisting behaviors during fights (Fig. 14c)[14]. Since both chemogeneci and optogenetic astrocyte stimulation did not increase pushing behavior (Fig. 3c, Fig. 5c, and Fig. 14c), I expected dmPFC neuron stimulation to confer dominance over astrocyte stimulation in the tube test between these two groups. However, unexpectedly, the winning rate was similar between the two groups (Fig. 14e and g). This finding indicates that resistance behavior is sufficient to assert dominance. According to a previous study, increased firing rate in pyramidal neurons in layer V of the dmPFC has a strong correlation with both pushing and resisting behavior during the tube test, and, as a result, these behavioral strategies lead to winning[14]. Although the higher firing rate or excitability of neurons induces more pushes and resistance

actions, our data show that only resistance behavior is elicited by astrocyte activity. Optogenetic astrocyte activation did not increase the neuronal excitability, but rather increased mEPSC amplitude and frequency, which might underlie the differences in behavioral outcome between neural vs. astrocyte stimulation. This suggests that increasing neuronal excitability and the strength of synaptic inputs into pyramidal neurons can differentially regulate dominance behavior mode (offensive pushing behavior vs. defensive resisting behavior). My findings concerning the function of dmPFC astrocytes in mouse resistance behavior will hopefully help to elucidate the brain functioning mechanisms of human endurance and patience in the future.

Studies on the molecular mechanisms indicate that elevated AMPA receptor expression levels in the dmPFC pyramidal neurons are responsible for the dmPFC synaptic potentiation and the subsequent change in mouse dominance behavior. For instance, AMPA receptor upregulation by injection of GluA4-expressing virus increases social rank in mice[13], and a reduction of AMPA receptors in neonatal mice by long-term isolation decreases social rank[127]. It has also been reported that phosphorylation of AMPA receptors by stress or fluoxetine[121] and allosteric modulation of AMPA receptors[128] can modulate social dominance. Furthermore, one recent study identified that long non-coding RNA (lncRNA) directly regulates AMPA receptor expression in dmPFC pyramidal neurons and thereby affects mouse dominance behaviors[129]. In line with these reports, our study revealed that dmPFC astrocyte-stimulated rank-4 mice showed increased surface GluA1 expression (a subunit of AMPA receptor) comparable to that of rank-1 mice. Accordingly, there was an increase in mEPSC amplitude in

rank-4 mice who received dmPFC astrocyte stimulation. My findings indicate that AMPA receptor expression in dmPFC pyramidal neurons can be modulated not only by MD-PFC neural activation, but also by dmPFC astrocyte activation. This also suggests that dmPFC astrocyte activation might be involved in the elevated AMPA receptor expression by repeated winning, which warrants future investigation.

For clear understanding of the role of dmPFC astrocyte in dominance behavior, *in vivo* functions of dmPFC astrocyte is needed to be investigated. First, in *ex vivo* slice electrophysiology experiment, I observed significantly increased excitatory synaptic inputs into pyramidal neurons. However, considering that reduced activity of inhibitory interneurons in dmPFC results in enhanced mouse dominancy[108], it should be observed the influences of optogenetic or chemogenetic astrocyte activation on not only excitatory functions but also inhibitory synaptic properties. Also, measuring a local field potential activity which indicates integrated excitatory and inhibitory neuronal activity might be helpful to identify the role of astrocyte. Second, although submissive mice showed significantly increased resistance behavior (time resisting) by dmPFC astrocyte stimulation in this study, however, whether spontaneous dmPFC astrocyte activity is occurred when the mice show resistance behavior during tube test is also necessary to be investigated. For this, performing *in vivo* two-photon Ca^{2+} imaging experiment may help to identify the involvement of dmPFC astrocyte cell in resistance behavior during the tube test. Taken together, various *in vivo* experiments must be conducted in the future study for clear identification of the role of dmPFC astrocyte in mouse dominance behaviors.

It should be noted that the optogenetic manipulation I employed is not physiological astrocyte activation. In particular, a recent study argues that optogenetic astrocyte activation may affect excitability of neurons nearby by increasing extracellular K^+ concentration in striatum region[130]. Although it is not clear how optic stimulation of ChR2-expressing astrocytes affects their physiology, I would like to propose that the behavioral and electrophysiological effects of optogenetic astrocyte activation in our study are not merely due to elevated potassium levels, because I did not observe any alteration in neuronal excitability upon optogenetic astrocyte stimulation (Fig. 2c and d). Also, chemogenetic astrocyte activation, which is more physiologically relevant, induced comparable behavioral and electrophysiological changes. Therefore, I would like to argue that the behavioral effects of dmPFC astrocyte stimulation may have physiological relevance.

Although patience or endurance is an important behavioral feature characterizing one's personality, no biological mechanisms have been proposed. In this regard, my data may shed new light on our understanding of the brain functioning mechanisms of patience or delay of gratification. Notably, endurance and patience can be important factors in pursuing a dominant status in human society. Individuals compete for status not by bullying and intimidating others, but by behaving in ways suggesting high levels of endurance and patience within the group[131]. Possibly, my observation of mouse resistance behavior upon dmPFC astrocyte stimulation, which was different from neuronal modulation, provides a novel and strategic way to solve social and psychological problems related to a lower social hierarchy by targeting dmPFC astrocytes.

Chapter II

The effects of dmPFC astrocyte activation-induced dominancy on depression

Abstract

Across species, social position in society can have large effects on health and diseases. Individuals with low social status are more vulnerable to MDD. Studies using postmortem brain of MDD patients have implicated astrocyte cells in dmPFC, however, their involvement in affective disorders due to submissiveness has not been studied.

Here, I investigated whether chemogenetic dmPFC astrocyte stimulation to chronic restraint stress (RS)-induced mice show both increased dominancy and amelioration of depressive behavior. After 3 weeks of RS, the mice showed depressive-like behavior compared from normal control. Chemogenetic stimulation of dmPFC astrocyte activation in RS mice induced winning in social competition in tube test by increasing the persistence of defensive behavior such as resistance. Furthermore, repetitive winning experience due to chemogenetic dmPFC astrocyte stimulation rendered rapid anti-depressant effect to chronic stress-induced depressive mice. I also tested whether optogenetic dmPFC pyramidal neuron stimulation could also change dominancy and depressive-like behaviors of RS mice, however, these mice did not show anti-depressive effect after the tube test, although they showed increased dominancy compared from normal mice.

In this chapter, dmPFC astrocyte-stimulated dominance behavior induces winning and finally affects depressive behavior of RS mice which is more effective than dmPFC pyramidal neuron-stimulation. It may give a clinical implication to treat depression due to lower social status in human.

Key words: Major depressive disorder (MDD), Restraint stress, Anti-depressant, Astrocyte, Dominance behavior

Introduction

More than 300 million people suffer from MDD, and it is the most prevalent mental health problem in the current society world-wide. MDD is often described as an overwhelming sadness, despair, and helplessness which lasts for several months or even years[132]. Individuals with MDD are at a high risk of suicide, with more than 90% of those who die by suicide who have a history of self-harm[133]. Due to the debilitating nature of MDD, most research has been focused on the identification of its etiology.

Current studies of depression are arguing and largely focusing on the identification of novel structures and functions of neural circuits of the brain[134]. For instance, optogenetic activation of dmPFC to dorsal raphe nucleus (DRN) circuit improves mouse depressive behaviors[135]. In this study, the mice showed increased kick frequency during forced swim test which is considered as an increased active coping behavior. Moreover, activation of serotonergic neurons in DRN which projects to somatostatin-expressing neurons in central nucleus of amygdala regulates mouse depressive behaviors[136]. Although these studies provide key neural substrates regulating depressive symptom, however, it is long way to go to reach clinical applications. Considering that depression is very complex disorder which is affected by various environmental or genetic factors, it is crucial to find a clear main cause of MDD to improve treatment efficiency.

Chronic stress is one of the main cause of depressive disorder. It affects various parts of animal body and causes diverse physiological changes, which are manifested in symptoms such as headache, stomachache, heartburn, fatigue,

overeating, or undereating[137] in humans. Severe and long-lasting adverse effects induced by chronic stress result in psychiatric disorder such as MDD[137,138]. Among various types of chronic stresses, in particular, a common factor that is pervasively linked to MDD is socio-economic status (SES), with substantial evidence that the more disadvantaged are disproportionately affected by mental health problems and their consequences. Moreover, SES is currently considered as one of the strongest predictors of mortality and mobility in humans, which that low SES is associated with higher risk of diseases including cardiovascular disease, cancer, and multiple psychiatric conditions[139]. In particular, MDD has been highly associated with low SES even after accounting for life style factors. In addition, individuals with low SES are more vulnerable to MDD[140,141], for low SES is a kind of chronic stress for human. Therefore, comorbidity between low social status (low SES) and depression is increasingly recognized.

Although the comorbidity between low social status and depression has been provided in human, a link between depressive and submissive behaviors was implied by an animal study using selective serotonin reuptake inhibitors (SSRIs)[121], widely used anti-depressant drugs for MDD. In this study, chronic SSRI administration not only reversed depressive behaviors of chronic stress-induced mice, but also rescued submissive behaviors[121]. Notably, chronic SSRI treatment rescued the astrocyte cell loss in the dmPFC of the depressive mice[58], which is often observed in MDD patients[142,143]. This suggests that dmPFC astrocytes may play a role in the psychological influence of social dominance. It is conceivable that dmPFC astrocyte may have a key role for the regulation of comorbidity of

dominance and depression, however, the role of dmPFC astrocyte in depressive and social dominance behaviors have still not been investigated.

Moreover, considering that depression have comorbidity with submissiveness[144] and submissive mice show depressive behaviors compared from dominant mice[31], there is no study investigating the possibility of anti-depression by dominancy increase. According to the previous report suggesting that repeated winning experience induces 'winner effect'[14], it is possible to think that repeated experience of winning may positively affect to psychological traits such as depressed mood. Because both dmPFC pyramidal neurons and astrocytes are all induce winning in the tube test which are shown in chapter I, therefore, performing tube test with optogenetic or chemogenetic activation of dmPFC pyramidal neuron of astrocytes. Taken together, make submissive mice into dominant is suitable for measure anti-depressive effect of chronic stress-induced depressive mice.

In the previous chapter, I revealed that dmPFC astrocyte activation induces hierarchical rank elevation of submissive mice. Here, in chapter II, I postulated that repetitive winning experience may induce psychological change, therefore, I compared depressive-like behavior before and after the winning of chronic restraint stressed mice to see whether depressive symptom can be ameliorated by changing the behavior mode. Lastly, I quantitatively determined the change of depressive-like phenotypes of stressed mice after winning by mathematical approach.

Materials and Methods

Animals

Six to 16-week-old male C57BL/6J mice of similar body weights were used for experiments. The animals were housed and maintained in a controlled environment at 22-24°C and 55% humidity with 12 h light/dark cycles and fed regular rodent chow and tap water ad libitum. All animal care was guided by the Seoul National University Institutional Animal Care and Use Committee (SNU IACUC, SNU-180416-3).

Stereotaxic Viral delivery

Nine to 10-week-old wild type male mice that showed stable hierarchy in cages were used for viral delivery. Animals were anesthetized with isoflurane and secured in a stereotaxic frame (Stoelting Co., Wood Dale, IL, USA). Holes the size of the injection needle were drilled into the skull, and bilateral or unilateral injections with 0.7 μl (titer 10^{13} GC/ml) of AAVDJ or AAV5 were administered in each side. The injection syringe (Hamilton Company, Reno, NV, USA) delivered the AAVDJ or AAV5 at a constant volume of 0.1 μl/min using a syringe pump (Stoelting Co.). The needle was left in place for 3 min after each injection to minimize the upward flow of the viral solution after raising the needle. The injection coordinates of the PL subregion of the dmPFC were angle: 10°, AP: +2.43, ML: ±0.61, DV: -1.78 from bregma. Mono fiber-optic cannula were bilaterally implanted 1 week after the viral injection, 400 μm above the viral injection site (angle: 10°, AP: +2.43, ML: ±0.61, DV: -1.38 from bregma). Anchor screws were located in the skull and fixed

with Zinc Polycarboxylate dental cement. AAVDJ-GFAP-mCherry, AAVDJ-CamKII-eGFP and AAVDJ-CamKII-ChR2-eGFP were purchased from the Korea Institute of Science and Technology (KIST, Seoul, Korea), and pXac2.1-gfaABC1D-hM3Dq-mCherry plasmid was purchased from Addgene (#92284, Watertown, MA, USA) and packaged in AAV5 by Upenn Vector Core (Philadelphia, PA, USA). Animals injected with virus were used for assessments of behaviors 2-3 weeks after the injection. Animals injected with AAVDJ or AAV5 but showing no detectable viral expression in the target region were excluded from the analyses.

Chronic restraint stress

Mice were individually placed into 50 ml polypropylene conical tubes with a nose-hole for ventilation, and were exposed to restraint stress (3 h/day) for 14 consecutive days. After restraint stress, mice were returned to the home cage. One day after the last restraint stress, mice were weighed and used for further experiments.

Behavioral studies

On the day of all behavioral testing, animals were moved to the test room and left to habituate for at least 1 h. The light condition of the test room was maintained at the same intensity (100 lux) as the animal rooms under daylight conditions.

Tube test. We used a transparent Plexiglas tube with 30 cm length and 3 cm inner diameter. Six-week-old male mice were housed in groups of 4 for at least 2 weeks before tube test. Before the main test, each mouse was trained to go through the

tube for 10 trials in two consecutive days. On the test day, pairs of mice were released into the opposite ends and met at the middle of the tube. The tube test was performed for 2 min. If no winner or loser was decided within 2 min, the test was repeated. Between each trial, the tube was cleaned with 70% ethanol. Within each cage of four pairs, mice were randomly assigned such that each mouse would meet every other mouse of the group only once, resulting in six matches per cage. All 6 pairs of mice were tested daily with a round robin design and ranks were determined by total number of wins. Only cage mates that maintained stable ranks for at least 3 or 4 days were used for further experiments. The behaviors were videotaped and both push and resistance behaviors were counted.

Tube test with chemogenetic astrocyte stimulation and optogenetic pyramidal neuron stimulation. After 2 days of tube training, CNO (3 or 6 mg/kg) was intraperitoneally injected to hM3-expressing mice. Then we performed tube test at 30 min, 2, 6, and 24 h after the injection. Identically, optogenetic stimulation (473 nm, 100 Hz, 1 ms of pulse duration) was delivered to ChR2-expressing mice.

Dominance competition between the mice groups (No stress vs. Stress). Each test mouse was matched 4 times against different group mice. The winning rate of each test mouse was calculated by counting total number of wins.

OFT. The apparatus consisted of a brightly illuminated 40 cm x 40 cm square arena surrounded by a 40 cm high wall. Mice were individually placed in the center of the arena, and their locomotion activity was monitored by an automatic system for 10 min. Light stimulation of 473 nm was intermittently turned on and off on the test mice (GFAP-ChR2 mice and GFAP-mCherry mice) with 1 min intervals. Total distance and time spent in the center zone per minute were analyzed by automated

video tracking system (SMART, Panlab SL, Barcelona, Spain). The activity chamber was cleaned with 70% ethanol after each use to eliminate any olfactory cues from the previously tested mouse.

FST and TST. We conducted forced swim tests by placing each animal individually in transparent cylinders filled with water (23-25°C; depth 15 cm) for 5 min. Immobility in the FST was defined as the state in which mice were judged to be making only the movements necessary to keep their head above the surface. The TST was performed by hanging each animal from the top of a square box for 5 min. For optogenetic astrocyte stimulation in FST, light was delivered during the whole experimental session to GFAP-ChR2 mice and their control group. Both trials were videotaped and immobility time was analyzed using a video tracking system.

Experimental protocols including OFT, FST, and TST were designed to take into account potential stress that could affect test mice behavior. Behavioral assessment was performed in the following sequential order to minimize stress effects: OFT, EPM, FST, and TST.

Pearson's correlation and K-means classification

K-means clustering analysis is one of the simplest and most popular unsupervised machine learning algorithms. It aims to separate scattered data into k clusters in which each data point belongs to the cluster with the nearest mean (centroid). This method has been successfully employed in various biological fields to identify and classify complex biological features[145-148].

We plotted individual mouse immobility values into a 2-dimentional space by defining M_n (t^{FST}, t^{TST}), in which M means mouse and n indicates the mouse number.

We first performed a Pearson's correlation analysis to verify whether the immobility values in the FST and TST correlated with each other. The FST immobility values of 56 mice, including all non-RS (n=28) and RS (n=28) mice, showed a significant positive correlation with the TST immobility values. We performed a K-means classification analysis to divide the immobility values into two groups (k=2). Classification was started from two random points for every cluster, and we performed 1000 iterative calculations to optimize the positions of the centroids in each cluster. After 1000 iterations, the centroids of each classified cluster were determined, and we compared the centroids with the values measured from experiments. Centroids of each classified group were similar to experimental values, and we then verified classification accuracy. The data were classified into 'Normal' and 'Depressed' groups with 91.1% classification accuracy. Among the 28 non-RS mice, 25 were correctly classified as "Normal" and 3 were incorrectly classified as "Depressed" (89.3% classification accuracy). Among the 28 RS mice, 26 were correctly classified as "Depressed" and 2 mice were incorrectly classified as "Normal" (92.9% classification accuracy). Next, we performed K-means classification using the FST and TST immobility values obtained from the non-RS and RS mice after tube testing. The k value was again 2, and the classification iteration was 1000. Both Pearson's correlation and K-means classification analyses were performed in MATLAB (R2019a).

Statistics

Satistical significance was determined using the two-tailed Student's t-test, paired t-test, Wilcoxon signed-rank test, or two-tailed Mann-Whitney U-test for

comparison between two groups. For multiple comparisons, one-way ANOVA and Bonferroni's multiple comparison tests were used. All data are represented as the mean ± s.e.m., and differences were considered statistically significant when the *p*-value was less than 0.05.

Results

Dominancy is related with depression.

Studies indicate a correlation between one's social status and susceptibility to depression[20,23,149]. Many studies show that chronic RS-induced depressive mice (RS mice) develop submissive behavior[31,121,150-152], and these behavioral phenotypes, i.e., depressive and submissive behaviors, are both rescued by chronic treatment with anti-depressants such as fluoxetine[31,121,152]. Considering the frequent comorbidity of submissiveness and depression, we explored whether the dmPFC astrocyte- or neuron-activated dominance behavior could affect RS-induced depressive-like behavior. We designed a behavioral paradigm to assess whether allowing tube test winning experiences by chemogenetic astrocyte (Fig. 1a) or optogenetic pyramidal neuron (Fig. 1b) activation in dmPFC could render anti-depressive effects to the RS mice. Mice were injected with gfaABC1D-hM3Dq (Fig. 1a, RS mice) or CamKII-ChR2 (Fig. 1b, RS mice) virus into the right PL region for chemogenetic astrocyte and optogenetic neuron stimulation, respectively. We adopted a chemogenetic astrocyte activation method for these experiments since it is more physiologically relevant than optogenetic activation. For the control, mice were injected with AAV5-gfaABC1D-mCherry or AAVDJ-CamKII-eGFP, and these control mice were not subjected to RS (non-RS mice). After 3 weeks of daily RS, mice were assessed for depressive-like behaviors in the OFT, FST, and TST (indicated as 'Pre-tests' in Fig. 1a and b). Following two consecutive days of tube training and a tube test (basal test), mice were subjected to tube tests with chemogenetic astrocyte stimulation with CNO injection (day 42–

43 in Fig. 1a) or optogenetic neuron stimulation (day 49–53 in Fig. 1b). All experimental mice were then re-assessed in the FST, TST, and OFT (indicated as 'Post-tests' in Fig. 1a and b).

Astrocyte stimulation-induced winning experiences render a rapid anti-depressive effect.

In the Pre-tests, RS mice exhibited levels of locomotive activity comparable to non-RS control mice (Fig. 2a). However, they showed significantly increased immobility in the FST and TST (Fig. 2b and c) compared with non-RS mice, indicating development of depressive-like behavior upon 3 weeks of daily RS. The day after the TST, we performed tube test training and a basal tube test to measure relative dominance between the two groups ('RS' vs. 'non-RS'). In this basal tube test, the non-RS mice had a higher winning rate than the RS mice and exhibited greater pushing and resistance behaviors (Fig. 3a-c, and Fig. 4a-c). On the following day, we performed the tube test again after dmPFC astrocyte stimulation via CNO injection (i.p., 6 mg/kg). Upon chemogenetic dmPFC astrocyte stimulation, the RS mice showed dramatically elevated resistance behavior both at 2 and 6 h, which increased their winning rates against the CNO-injected non-RS control mice (Fig. 3b and c). Of interest, after 24 h, the astrocyte-activated RS mice increased pushing behavior as well (Fig. 3a). At 6 and 24 h after CNO injection, the winning rate of the RS mice was higher than that of the non-RS mice (Fig. 3c). Meanwhile, optogenetic stimulation of dmPFC neuron in RS mice rendered different behavioral outcomes. Contrary to astrocyte stimulation, dmPFC pyramidal neuron-stimulated RS mice did not win out over the light-stimulated

non-RS control mice, although both pushing and resisting times gradually increased by repeated tube tests (Fig. 4). The neuron-stimulated RS mice exhibited a winning rate comparable to non-RS mice only after 3 days (Fig. 4c).

After tube tests, we repeated the FST, TST, and OFT ('Post-tests'). Locomotive behavior was not affected by winning experiences in both dmPFC astrocyte- and pyramidal neuron-stimulated RS mice (Fig. 5a). In RS mice who obtained tube test winning experiences by dmPFC astrocyte activation, the depressive behaviors observed in the 'Pre-tests' were almost completely abrogated (Fig. 5b and c). However, RS mice who increased their winning rate by optogenetic dmPFC pyramidal neuron stimulation still showed higher immobility in the FST and TST during 'Post-tests' compared to non-RS controls (Fig. 5a-c). These data indicate that dmPFC astrocyte activation, but not neuron stimulation, renders anti-depressive effects to RS mice.

Acute chemogenetic astrocyte stimulation does not affect depressive behaviors of RS mice.

To test the relationship between winning experience acquisition and anti-depressive effects by dmPFC astrocyte activation, we subjected the gfaABC1D-hM3Dq virus- or GFAP-mCherry virus-injected mice to the same experimental scheme except for the tube tests (Fig. 6a). Notably, chemogenetic dmPFC astrocyte stimulation per se, without tube test winning experiences, did not induce anti-depressive effects in RS mice (Fig. 6b-e), indicating that tube test winning experiences are required for the dmPFC astrocyte-derived anti-depressive effects. In line with this, acute chemogenetic dmPFC astrocyte stimulation did not deter the

RS mice from manifesting depressive-like behavior in the FST compared with non-RS control mice (Fig. 7).

K-means clustering analysis confirms the anti-depressive effects of dmPFC astrocyte-derived winning experiences.

To quantitatively determine the development of depressive-like phenotypes of RS mice after winning, I performed a K-means clustering analysis, a widely used mathematical analysis to categorize complex data sets into various subgroups[153,154] (Fig. 8a). K-means clustering analysis is one of the simplest and most popular unsupervised machine learning algorithms. It aims to separate scattered data into *k* clusters in which each data point belongs to the cluster with the nearest mean (centroid). This method has been successfully employed in various biological fields to identify and classify complex biological features[145-148].

I performed K-means clustering analysis to classify the values into two groups, 'Normal' and 'Depressed'. The K-means clustering algorithm successfully classified the FST and TST values from non-RS mice and RS mice with 89.3% and 92.9% classification accuracy, respectively (Fig. 8b). Only three of 28 non-RS mice and two out of 28 RS mice were incorrectly classified as 'Depressed' and 'Normal', respectively (Fig. 8b). Combining the values of both non-RS and RS mice together, the classification accuracy was 91.1% (Fig. 8c). The centroids of each group ('Normal' or 'Depressed') were similar to the mean immobility time of non-RS and RS mice (Fig. 8d).

I plotted all immobility values from 'Pre- tests' of FSTs and TSTs of all tested mice and found a significant positive correlation of immobility time between the FST

and TST (R^2=0.4073) (Fig. 9a). Individual data clearly show that mice with high immobility in the FST also exhibit high immobility in the TST (Fig. 9a). I then analyzed immobility data of the FST and TST from 'Post-tests' of RS mice. The results showed that all RS mice who obtained winning experiences by dmPFC astrocyte stimulation were classified 'Normal' (Fig. 9b). In contrast, only one RS mouse with dmPFC pyramidal neuron stimulation was classified as 'Normal' (14.3%), while 7 out of 8 mice were still classified as 'Depressed' (85.7%) (Fig. 10). Taken together, these results confirm the anti-depressive effects of dmPFC astrocyte-stimulated winning experiences and demonstrate that tube test winning from targeting dmPFC astrocytes renders more effective anti-depressive effects than targeting dmPFC pyramidal neurons (Fig. 11).

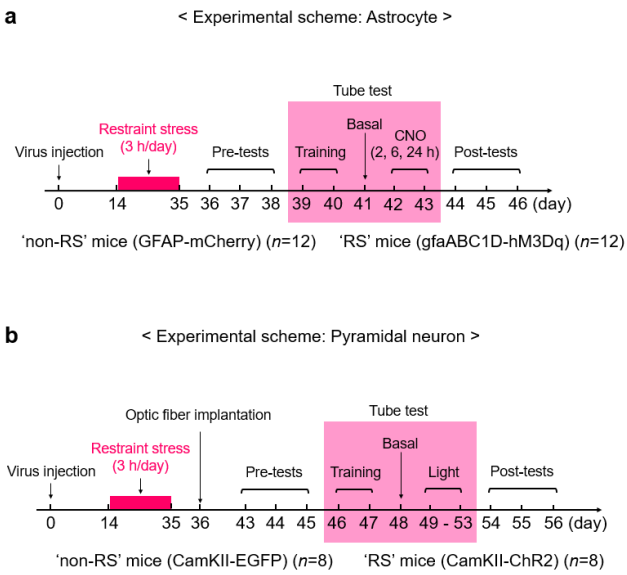

Figure 1. Experimental schemes to measure winning-induced anti-depressive effect. a, Behavioral experimental scheme targeting dmPFC astrocytes. The experimental schemes were designed to compare depressive behaviors of RS mice before and after the tube test. Two weeks after virus injection (*n*=12 for AAVDJ-GFAP-mCherry in 'non-RS' mice and *n*=12 for AAV5-gfaABC1D-hM3Dq-mCherry in 'RS' mice), 3 hours of daily restraint stress was delivered to RS mice for 3 weeks. The day after the last restraint stress, the OFT, FST, and TST (indicated as 'Pre-tests') were performed for 3 consecutive days. Following 2 days of tube training, mice were subjected to a basal tube test and then a tube test following CNO treatment (2, 6, and 24 h after CNO injection). After the last day of the tube test, the FST, TST, and OFT were performed again (indicated as 'Post-tests'). **b**, Behavioral experimental scheme targeting dmPFC pyramidal neurons. Two weeks after virus injection (*n*=8 for AAVDJ-CamKII-eGFP in 'non-RS' mice and *n*=8 for AAVDJ-CamKII-ChR2-eGFP in 'RS' mice), restraint stress was delivered to RS mice for 3 weeks. After the last day of restraint stress, optic fiber was implanted in all mice. One week later, the groups were given 'Pre-tests' (OFT, FST, and TST). Following 2 days of tube training, mice were subjected to tube tests with light stimulation. Then, the groups were given 'Post-tests' (FST, TST, and OFT).

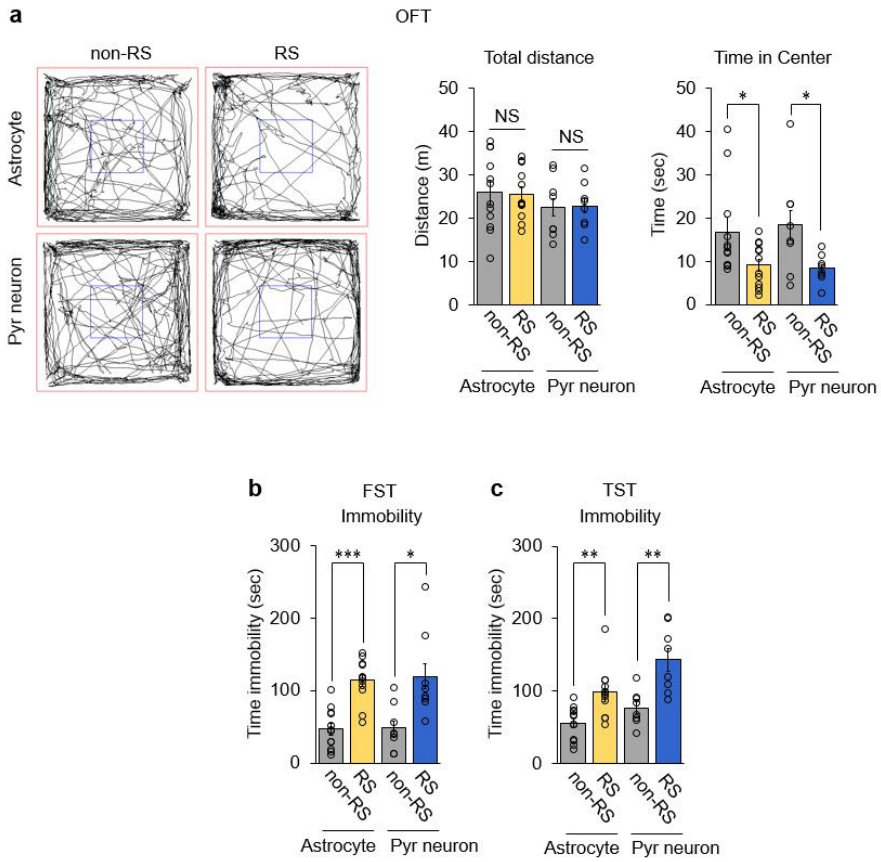

Figure 2. Chronic restraint stress induces increased depressive-like behaviors. **a**, Traces of locomotion, total distance traveled, and time in center in OFT. Student's *t*-test. **b**, Time immobility in FST. Student's *t*-test. **c**, Time immobility in TST. Student's *t*-test. *p<0.05; **p<0.01; ***p<0.001; NS, not significant. Data are presented as the mean ± s.e.m.

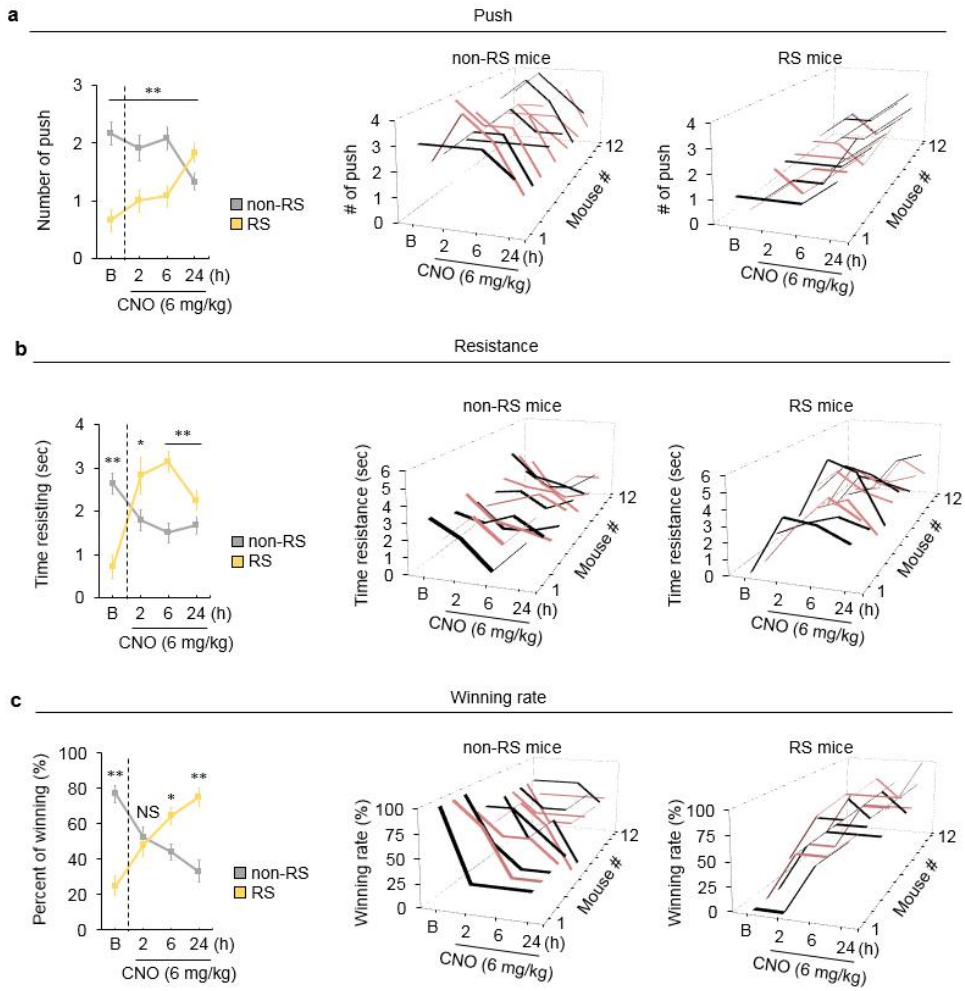

Figure 3. Behavioral mode shifts of RS mice by dmPFC astrocyte activation. a and **b**, Comparison of pushing and resistance of 'non-RS' and 'RS' mice during the tube competition before and after CNO injection (6 mg/kg, i.p.). Student's *t*-test. **c**, Percent of winning between 'non-RS' and 'RS' mice before and after CNO injection. Paired *t*-test. *p<0.05; **p<0.01; NS, not significant. Data are presented as the mean ± s.e.m.

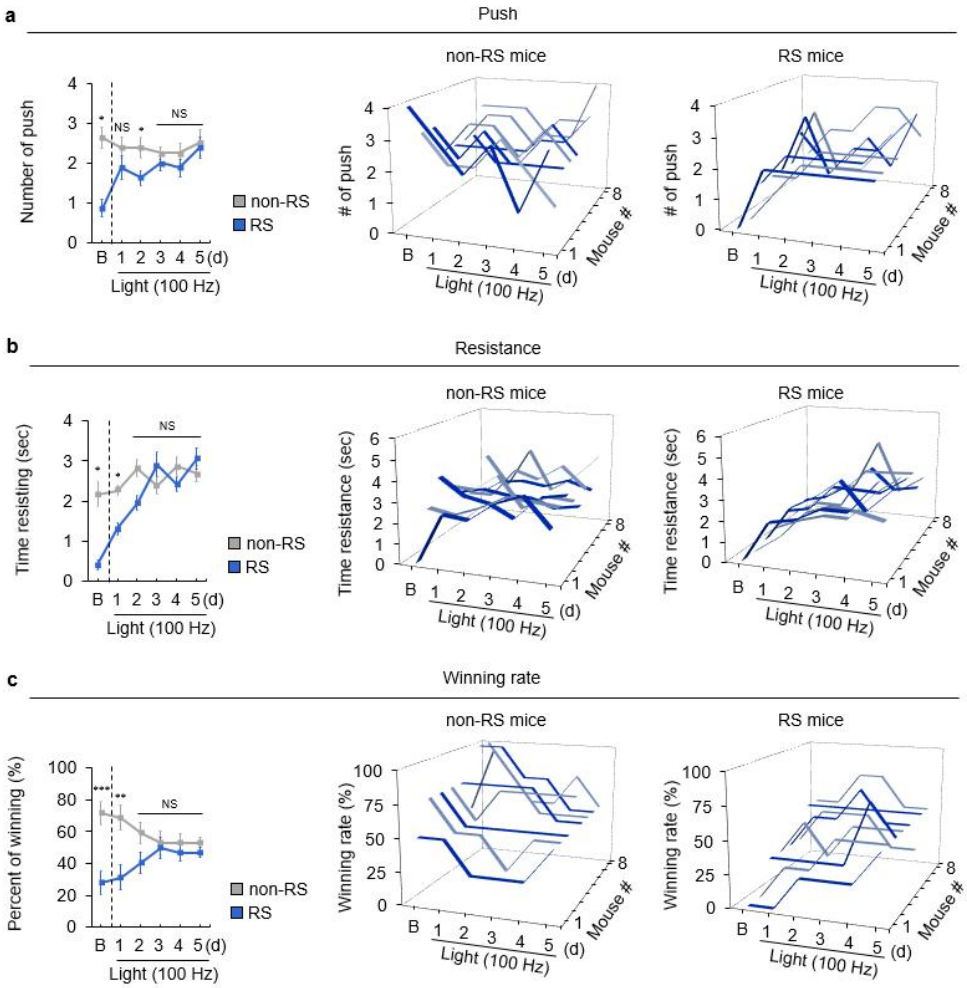

Figure 4. Behavioral mode shifts of RS mice by dmPFC pyramidal neuron-activation. a and **b**, Comparison of pushing and resistance of 'non-RS' and 'RS' mice during the tube competition before and after light stimulation (473 nm, 100 Hz). Student's *t*-test. **c**, Percent of winning between 'non-RS' and 'RS' mice before and after light stimulation. Paired *t*-test. *p<0.05; **p<0.01; ***p<0.001; NS, not significant. Data are presented as the mean ± s.e.m.

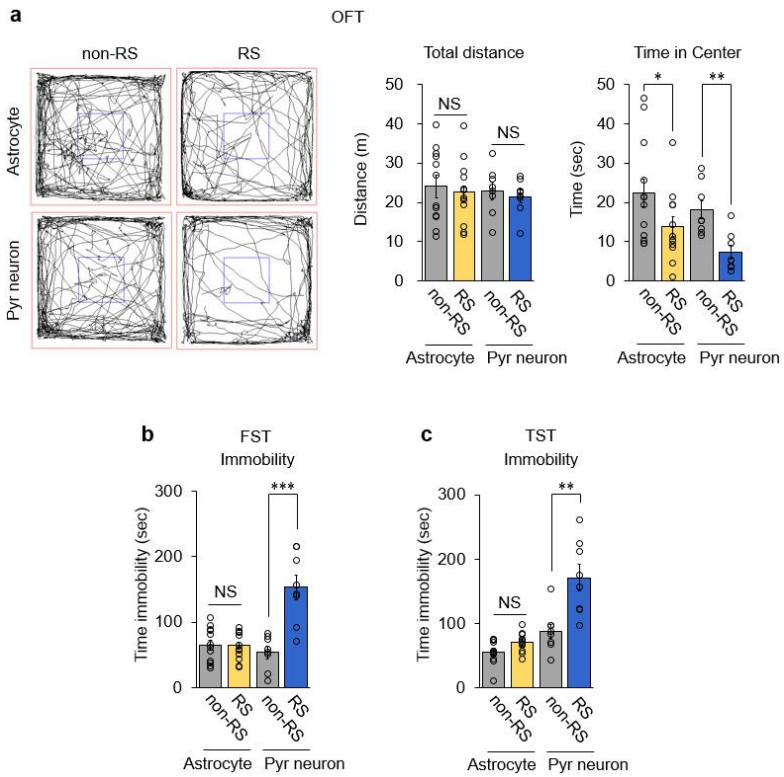

Figure 5. Winning experience with resistant behavioral strategy in the tube competition has a rapid anti-depressant-like effect on chronic restraint stress-induced depression. a, Locomotive behaviors of non-RS and RS mice. Student's *t*-test. **b**, Time immobility from FST after the tube test after the tube test. Student's *t*-test. **c**, Time immobility from TST after the tube test in experimental set #1. Student's *t*-test. *p<0.05; **p<0.01; ***p<0.001; NS, not significant. Data are presented as the mean ± s.e.m.

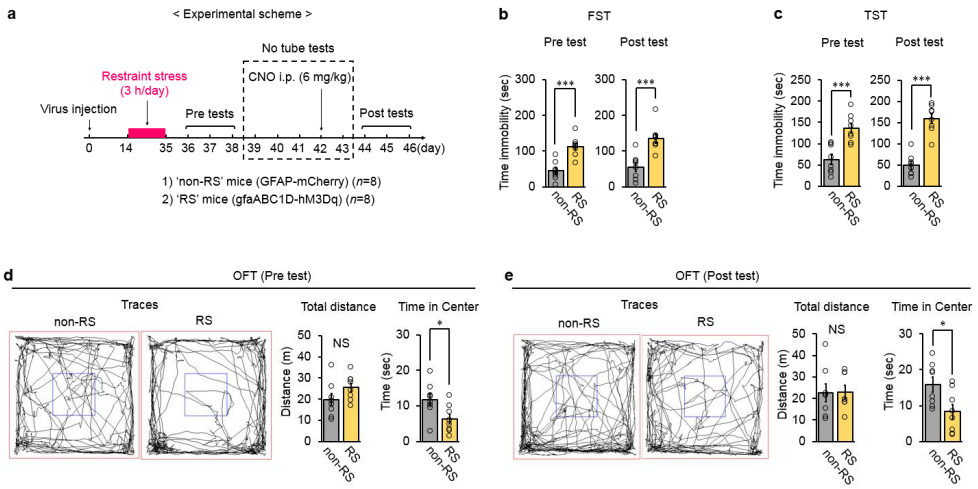

Figure 6. dmPFC astrocyte activation-derived anti-depressive-like behaviors were not observed in the absence of tube test winning experiences. a, Experimental scheme to measure the effects of tube test winning experience on the anti-depressive-like behaviors shown in the dmPFC astrocyte-activated RS mice. RS mice were subjected to the same experimental procedures as Figure 5a, but without tube tests. **b** and **c,** Depressive-like behaviors of RS and non-RS mice were measured by comparing 'Pre-tests' (FST at day 37 and TST at day 38) and 'Post-tests' (FST at day 44 and TST at day 45). RS mice showed higher immobility times than non-RS control mice before and after CNO injection (6 mg/kg, i.p.). Student's *t*-test. **d** and **e**, Mouse locomotion measured by OFT before (Pre-test at day 36) and after (Post-test at day 46) CNO injection. Student's *t*-test. *p < 0.05; ***p<0.001; NS, not significant. Data are presented as mean ± s.e.m.

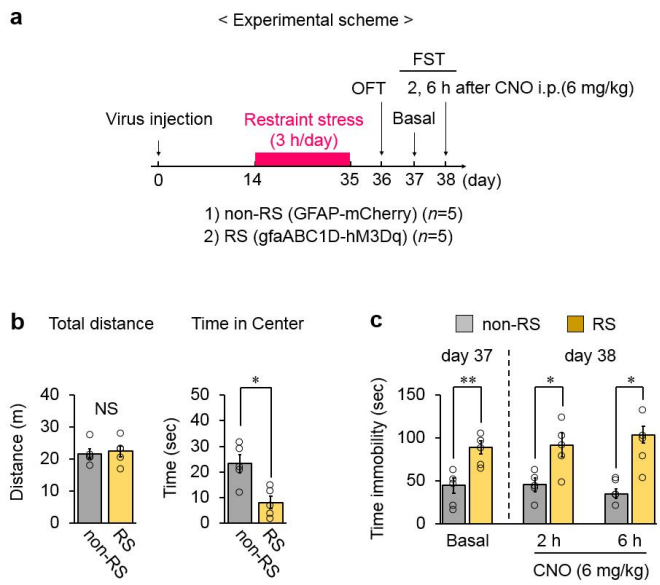

Figure 7. Acute dmPFC astrocyte activation does not induce anti-depressant effect. a, Experimental scheme to measure anti-depressive behavior of RS mice after acute CNO injection. AAVDJ-GFAP-mCherry or AAV5-gfaABC1D-hM3Dq-mCherry virus was injected into dmPFC (day 0). After 3 weeks RS, OFT and FST were performed to measure basal locomotion (day 36) and depressive behavior (day 37). At day 38, FST was performed again at 2 and 6 h after the CNO injection (6 mg/kg). **b**, The result of (*Right*) total distance and (*Left*) time in center from OFT. **c**, Time immobility measured by FST at basal, and 2 and 6 h after CNO injection. Student's *t*-test. *p < 0.05; **p < 0.01; NS, not significant. Data are presented as the mean ± s.e.m.

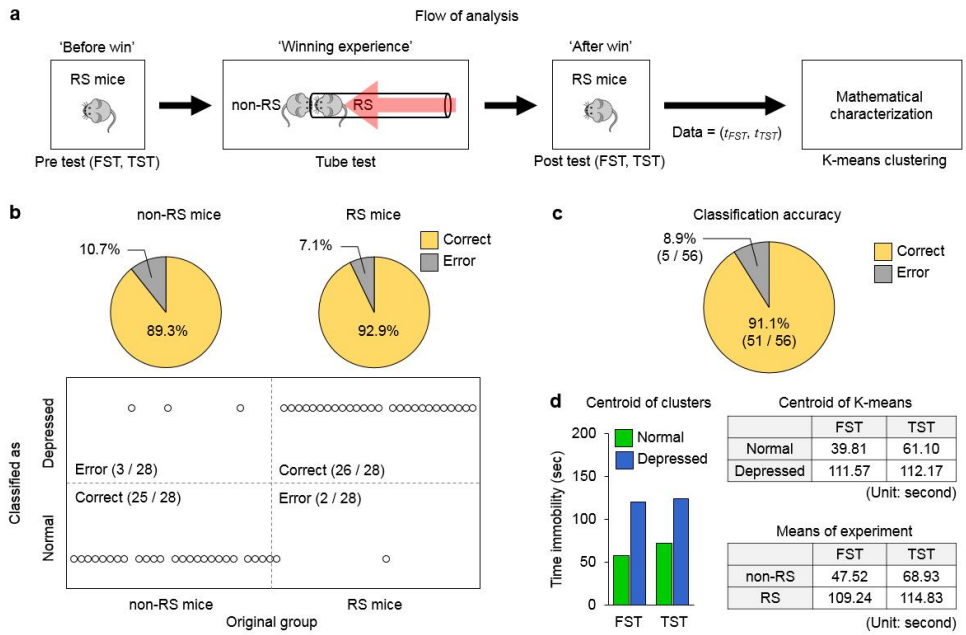

Figure 8. Astrocyte-derived winning experience has a 75% of anti-depressant effect in RS mice. a, Scheme of K-means clustering analysis. RS mice, which show both submissive and depressive phenotypes, were subjected to repeated tube tests with dmPFC astrocyte- or neuron-stimulation, allowing winning experiences. The immobility times in the FST and TST before ('Pre-tests') and after ('Post-tests') the tube tests were collected and analyzed by K-means clustering analysis. **b,** The data were clustered into 2 groups, 'Normal' and 'Depressed'. The immobility time values from Pre-tests (FST and TST) of non-RS and RS mice were used to classify the data into two groups. (n=28, data from Experiments in Figure 5a and b, and Supplemental Fig. 5c). Among 28 non-RS mice, 25 out of 28 mice were classified as 'Normal', and 3 out of 28 mice were classified as 'Depressed' (Classification accuracy = 89.3%). Among 28 RS mice, 26 out of 28 mice were classified as 'Depressed' and 2 mice were classified as 'Normal' (classification accuracy = 92.9 %). **c**, Combining both non-RS and RS mice, K-means clustering method classified the behavior data with 91.1% accuracy. Only 5 out of 56 mice were incorrectly classified (error rate = 8.9%). **d**, Centroids of each classified cluster were similar to the mean values of immobility measured from experiments.

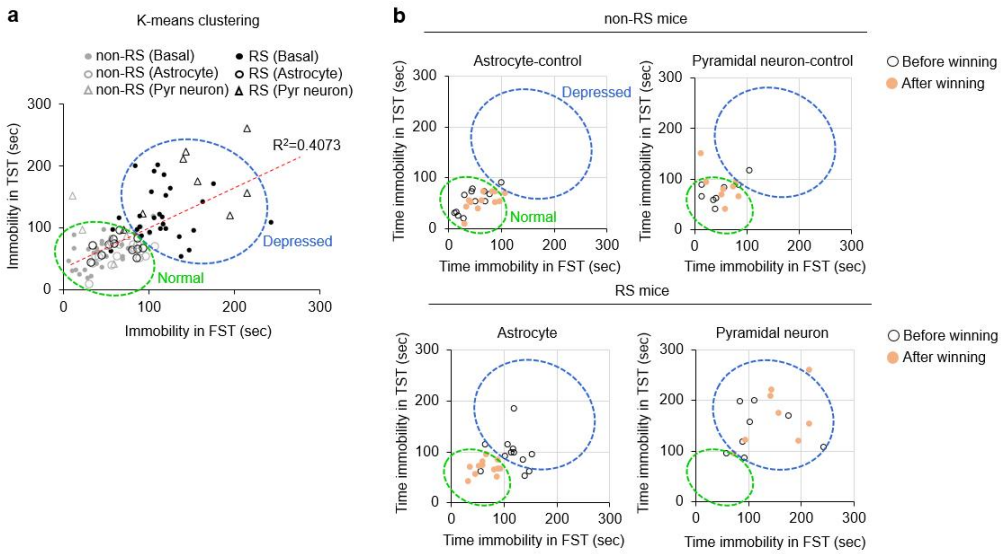

Figure 9. Behaviors of RS mice after repetitive winning are classified as non-RS-like behaviors by the K-means clustering analysis. a, Pearson's correlation analysis shows that the immobility values between the FST (n=28) and TST (n=28) show significant positive correlation (R^2=0.4073). The result of K-means clustering analysis classified the values into two groups (green: 'Normal', and blue: 'Depressed'). **b**, Individual scatter plots of immobility times of non-RS and RS mice measured from the FST and TST after tube tests. These scatter plots clearly show that immobility times from the FST and TST of astrocyte-stimulated RS mice are classified in the 'Normal' cluster; however, the data of neuron-stimulated RS mice are still classified in the 'Depressed' cluster.

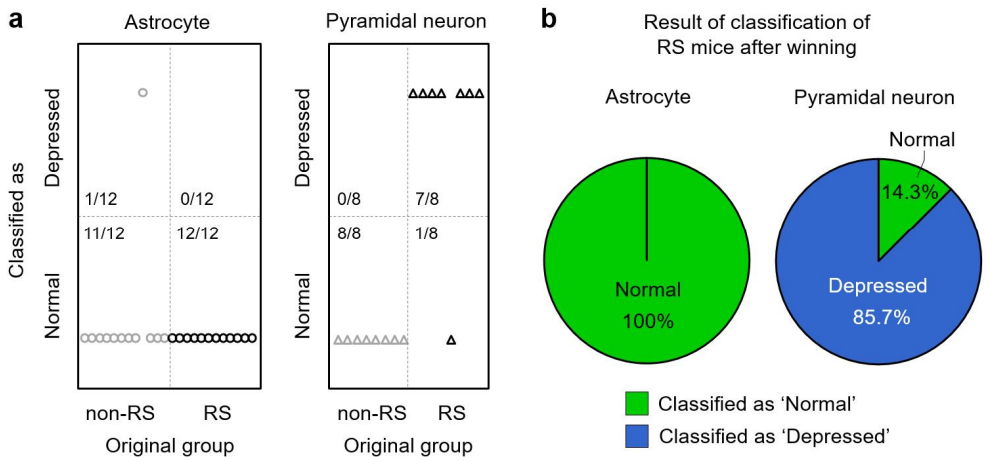

Figure 10. Astrocyte-induced winning renders rapid anti-depression. a, Results of the K-means clustering of RS mice who obtained winning experiences upon dmPFC astrocyte- or pyramidal neuron-stimulation. In astrocyte-stimulated RS mice, all 12 mice were classified as 'Normal'. In dmPFC pyramidal neuron-stimulated RS mice, only 1 of 8 mice was classified as 'Normal', and 7 mice were classified as 'Depressed'. **b**, Comparison of the percentages of classification of RS mice after winning experiences. Astrocyte-targeted RS mice were all classified as 'Normal' (100%; 12 out of 12) after tube tests. Pyramidal neuron-targeted RS mice were classified as 'Normal' (14.3%; 1 out of 8) or 'Depressed' (85.7%; 7 out of 8) after tube tests.

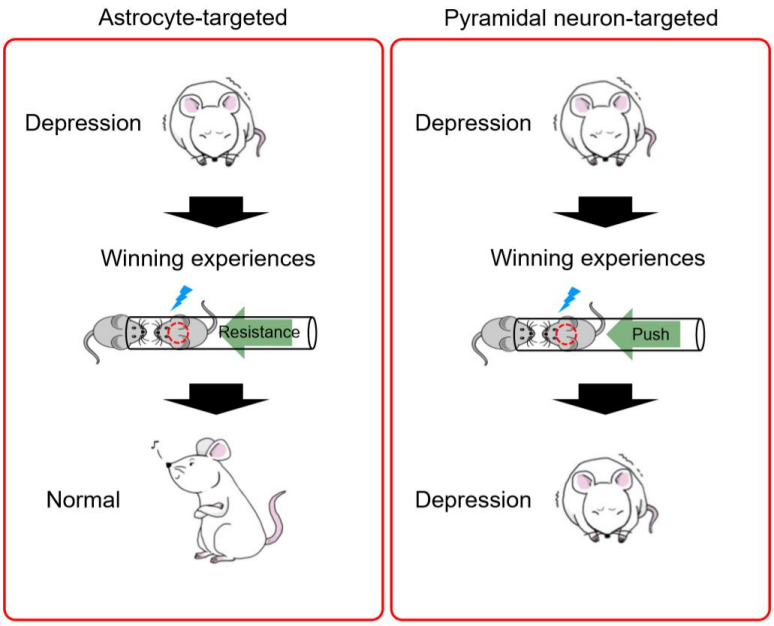

Figure 11. Graphical summary. Chronic restraint stress received mice show depressive-like behaviors. dmPFC astrocyte or pyramidal neuron stimulation of these mice induces resistance or pushing behavior respectively during the tube test, and it results in the winning against normal mice. dmPFC pyramidal neuron-stimulated stressed mice still show depressive phenotypes although they experienced winning. However, repeated winning experience of stressed mice by dmPFC astrocyte-stimulation show rapid anti-depressive behaviors.

Discussion

In this study, I uncovered a novel role of dmPFC astrocytes in controlling mouse dominance behavior, and subsequently a depressive behavior. I observed rapid anti-depressive effects by astrocyte-derived winning experience. In this study, the 'RS' mice started to win by resistance behavior, however, they showed significantly elevated pushing action at 24 h after the CNO injection. This behavioral shift may be due to the prior winning experience obtained by resistance action (2 and 6 h), which might confer a winning effect.

A causal relationship between low social status and depression has been proposed in clinical studies[25,152], yet it had not been investigated in animals. In this study, we failed to observe statistically significant depressive-like behavior in rank-4 mice compared to rank-1 mice (Fig. 5a). Therefore, as an alternative, we adopted an RS mouse model that showed both depressive and submissive behaviors to study the putative relationship between these two behaviors. First, we tested whether dmPFC astrocyte or neuron stimulation induces dominant behavior in the RS-induced depressive mice. As with un-stressed normal mice, dmPFC astrocyte stimulation increased resistance behavior of RS mice in tube test, while dmPFC neuronal stimulation increased both pushing and resistance behaviors. Of interest, upon repeated tube competition, chemogenetic activation of dmPFC astrocytes in RS mice elicited a dramatic behavioral mode change (from defensive resisting to offensive pushing) and reversed the final winning odds against non-RS control mice within a day. In contrast, optogenetic stimulation of dmPFC pyramidal neurons in RS mice caused a gradual increase of both pushing and resistance

behaviors but failed to reverse the final winning odds against non-RS mice even after five days. These data suggest that dmPFC astrocyte stimulation exerts more potent dominance-enhancing effects in depressed mice than dmPFC pyramidal neuron stimulation.

The most important finding of our study is that dmPFC astrocyte stimulation induced rapid and strong anti-depressive effects in RS mice. What is intriguing is that such astrocyte stimulation-derived anti-depressive effects were not observed in the absence of tube test winning. This indicates that dmPFC astrocyte activation per se is not sufficient, but rather winning experiences in the tube test are required for the anti-depressive effects. It has been proposed that repetitive winning experiences induce 'winning memory' and often result in 'winner effect'[155]. Although purely speculative, it can be conceived that repeated tube test winning experiences aided by dmPFC astrocyte stimulation helped to form 'winning memory' in the RS mice, which changed their depressive behavioral mode.

It needs to be noted that, contrary to astrocyte stimulation, optogenetic dmPFC pyramidal neuron stimulation failed to induce anti-depressive effects in RS mice, even though it increased the winning rate of RS mice to a level similar to that of non-RS mice after five days of consecutive tube tests. This might be simply because the final winning rate of these mice was not high enough to induce anti-depressive effects; dmPFC astrocyte-stimulated RS mice won out over non-RS mice in the tube tests, but neuron-stimulated RS mice did not. It is also possible that more than tube test winning is needed for the dmPFC astrocyte stimulation to induce anti-depressive effects. It is conceivable that dmPFC astrocyte activation

also has an influence on the function of other dmPFC neurons besides pyramidal neurons, which is required for the anti-depressive effects. Indeed, it has been reported that prefrontal inhibitory GABAergic neurons affect both mouse dominance[108] and depressive behavior[156,157]. In this regard, it will be of interest to test if dmPFC astrocyte activation also affects GABAergic neuron activity.

Self-awareness of submissiveness might be a key feature affecting depressive mood in subordinate subjects, which are often managed by cognitive behavior-based therapy (CBT) for depression[158,159]. Our data of the unexpected roles of dmPFC astrocytes in dominant and anti-depressive behaviors might lead to the elucidation of the biological basis of CBT for depression. It also needs to be noted that the anti-depressive behavior manifested within a day of astrocyte-stimulated tube test winning. Such a rapid anti-depressant effect from dmPFC astrocyte-derived winning experiences is quite remarkable considering that even SSRIs, traditional anti-depressant drugs, require several weeks or even months to exert their anti-depressive effects. Furthermore, considering the prevalent side effects of traditional anti-depressant drugs[89,160], this astrocyte activation-induced behavioral approach may be a much more efficient strategy for depression treatment. Although the precise cellular and molecular mechanisms underlying the anti-depressive effects of astrocyte-stimulated winning experiences remain elusive, our results could have clinical implications for treating depression caused by low social status by targeting astrocytes.

Conclusion

In this study, I revealed that dmPFC astrocytes induce winning in submissive mice by resistance behavior during tube test, and this behavioral mode shift reduces depressive-like phenotype of stress-induced depressive mice.

In chapter I, I chemogenetically and optogenetically stimulated dmPFC astrocyte of submissive mice which previously showed repeated losing. However, after dmPFC astrocyte stimulation, the mice showed increased resistant action. This dmPFC astrocyte-derived dominance behavior induced winning of submissive mice. As a mechanism, dmPFC astrocyte stimulation increased extracellular glutamate, and it showed correlation with AMPA receptor-mediated excitatory synaptic input. These results suggest that dmPFC astrocytes play crucial role for social winning by showing persistence of resistance behavior.

In chapter II, I revealed behavior-based treatment of depression. I introduced depressive mouse model by giving a chronic restraint stress. All stressed mice showed both depressive and submissive behaviors compared from their control mice. However, after chemogenetic stimulation of dmPFC astrocyte, stressed mice showed prolonged winning in tube test even after without dmPFC astrocyte stimulation. Behavioral actions were shifted from resistance to pushing. Such winning experience successfully reversed the depressive behaviors of stressed mice.

These results suggest that dmPFC astrocyte could be a novel target for the individual with low social status, and may provide a clinical implication in treating depression due to low social status.

References

1 Cummins, D. D. How the social environment shaped the evolution of mind. *Synthese* **122**, 3-28 (2000).

2 Boyce, W. T. Social stratification, health, and violence in the very young. *Ann Ny Acad Sci* **1036**, 47-68 (2004).

3 Sapolsky, R. M. Social status and health in humans and other animals. *Annu Rev Anthropol* **33**, 393-418 (2004).

4 Sapolsky, R. M. The influence of social hierarchy on primate health. *Science* **308**, 648-652 (2005).

5 Wheeler, L. Motivation as a Determinant of Upward Comparison. *J Exp Soc Psychol* **2**, 27-31 (1966).

6 Karafin, M. S., Tranel, D. & Adolphs, R. Dominance attributions following damage to the ventromedial prefrontal cortex. *J Cognitive Neurosci* **16**, 1796-1804 (2004).

7 Pratto, F., Sidanius, J., Stallworth, L. M. & Malle, B. F. Social-Dominance Orientation - a Personality Variable Predicting Social and Political-Attitudes. *J Pers Soc Psychol* **67**, 741-763 (1994).

8 Chen, T., Beekman, M. & Ward, A. J. W. The role of female dominance hierarchies in the mating behaviour of mosquitofish. *Biol Letters* **7**, 343-345 (2011).

9 Anacker, A. M. J. *et al.* Enhanced Social Dominance and Altered Neuronal Excitability in the Prefrontal Cortex of Male KCC2b Mutant Mice. *Autism Res* **12**, 732-743 (2019).

10 Arrant, A., Filiano, A., Warmus, B., Hall, A. & Roberson, E. A biphasic social dominance phenotype in progranulin-insufficient mice is associated With abnormal cell signaling and neuronal morphology in the amygdala and prefrontal cortex. *J Neurochem* **138**, 415-416 (2016).

11 Lea, A. J. *et al.* Dominance rank-associated gene expression is widespread, sex-specific, and a precursor to high social status in wild male baboons. *P Natl Acad Sci USA* **115**, E12163-E12171 (2018).

12 Easley, S. P., Coelho, A. M. & Rutenberg, G. W. Lipsmacking - an Indicator of Dominance Status in Baboons. *Am J Primatol* **14**, 418-419 (1988).

13 Wang, F. *et al.* Bidirectional Control of Social Hierarchy by Synaptic Efficacy in Medial Prefrontal Cortex. *Science* **334**, 693-697 (2011).

14 Zhou, T. T. *et al.* History of winning remodels thalamo-PFC circuit to reinforce social dominance. *Science* **357**, 162-+ (2017).

15 Kingsbury, L. *et al.* Correlated Neural Activity and Encoding of Behavior across Brains of Socially Interacting Animals. *Cell* **178**, 429-+ (2019).

16 Adler, N. *et al.* Social status and health: A comparison of British civil

servants in Whitehall-II with European- and African-Americans in CARDIA. *Soc Sci Med* **66**, 1034-1045 (2008).

17 Lorant, V. *et al.* Socioeconomic inequalities in depression: A meta-analysis. *Am J Epidemiol* **157**, 98-112 (2003).

18 McMillan, K. A., Enns, M. W., Asmundson, G. J. G. & Sareen, J. The Association Between Income and Distress, Mental Disorders, and Suicidal Ideation and Attempts: Findings From the Collaborative Psychiatric Epidemiology Surveys. *J Clin Psychiat* **71**, 1168-1175 (2010).

19 Euteneuer, F. Subjective social status and health. *Curr Opin Psychiatr* **27**, 337-343 (2014).

20 Hoebel, J., Maske, U. E., Zeeb, H. & Lampert, T. Social Inequalities and Depressive Symptoms in Adults: The Role of Objective and Subjective Socioeconomic Status. *Plos One* **12** (2017).

21 O'Connor, R. C. & Kirtley, O. J. The integrated motivational-volitional model of suicidal behaviour. *Philos T R Soc B* **373** (2018).

22 Wetherall, K., Robb, K. A. & O'Connor, R. C. An Examination of Social Comparison and Suicide Ideation Through the Lens of the Integrated Motivational-Volitional Model of Suicidal Behavior. *Suicide Life-Threat* **49**, 167-182 (2019).

23 Wetherall, K., Robb, K. A. & O'Connor, R. C. Social rank theory of depression: A systematic review of self-perceptions of social rank and their relationship with depressive symptoms and suicide risk. *J Affect Disorders* **246**, 300-319 (2019).

24 Zvolensky, M. J. *et al.* Subjective Social Status and Anxiety and Depressive Symptoms and Disorders among Low Income Latinos in Primary Care: The Role of Emotion Dysregulation. *Cognitive Ther Res* **41**, 686-698 (2017).

25 Langner, C. A., Epel, E. S., Matthews, K. A., Moskowitz, J. T. & Adler, N. E. Social Hierarchy and Depression: The Role of Emotion Suppression. *J Psychol* **146**, 417-436 (2012).

26 Cohen, S. & Pressman, S. D. Positive affect and health. *Curr Dir Psychol Sci* **15**, 122-125 (2006).

27 Salovey, P., Rothman, A. J., Detweiler, J. B. & Steward, W. T. Emotional states and physical health. *Am Psychol* **55**, 110-121 (2000).

28 Keltner, D., Gruenfeld, D. H. & Anderson, C. Power, approach, and inhibition. *Psychol Rev* **110**, 265-284 (2003).

29 Keltner, D., Young, R. C., Heerey, E. A., Oemig, C. & Monarch, N. D. Teasing in hierarchical and intimate relations. *J Pers Soc Psychol* **75**, 1231-1247 (1998).

30 Chen, X. N., Zhu, H., Meng, Q. Y. & Zhou, J. N. Estrogen receptor-alpha and -beta regulate the human corticotropin-releasing hormone gene

through similar pathways. *Brain Res* **1223**, 1-10 (2008).

31 Horii, Y. *et al.* Hierarchy in the home cage affects behaviour and gene expression in group-housed C57BL/6 male mice. *Sci Rep-Uk* **7** (2017).

32 Ferrari, A. J. *et al.* Burden of Depressive Disorders by Country, Sex, Age, and Year: Findings from the Global Burden of Disease Study 2010. *Plos Med* **10** (2013).

33 Berton, O. & Nestler, E. J. New approaches to antidepressant drug discovery: beyond monoamines. *Nat Rev Neurosci* **7**, 137-151 (2006).

34 Gao, Y. B., Li, L. P., Zhu, X. H. & Gao, T. M. [Recent progress in neurobiological mechanisms of depression]. *Sheng Li Xue Bao* **64**, 475-480 (2012).

35 Teo, A. R., Choi, H. & Valenstein, M. Social relationships and depression: ten-year follow-up from a nationally representative study. *Plos One* **8**, e62396 (2013).

36 Barger, S. D., Messerli-Burgy, N. & Barth, J. Social relationship correlates of major depressive disorder and depressive symptoms in Switzerland: nationally representative cross sectional study. *Bmc Public Health* **14**, 273 (2014).

37 Barger, S. D., Messerli-Burgy, N. & Barth, J. Social relationship correlates of major depressive disorder and depressive symptoms in Switzerland: nationally representative cross sectional study. *Bmc Public Health* **14** (2014).

38 Luciano, J. V. *et al.* Utility of the twelve-item World Health Organization Disability Assessment Schedule II (WHO-DAS II) for discriminating depression "caseness" and severity in Spanish primary care patients. *Qual Life Res* **19**, 97-101 (2010).

39 Capibaribe, V. C. C. *et al.* Thymol reverses depression-like behaviour and upregulates hippocampal BDNF levels in chronic corticosterone-induced depression model in female mice. *J Pharm Pharmacol* (2019).

40 Forte, A. *et al.* Long-term morbidity in bipolar-I, bipolar-II, and unipolar major depressive disorders. *J Affect Disord* **178**, 71-78 (2015).

41 Yao, W. *et al.* Effects of amycenone on serum levels of tumor necrosis factor-alpha, interleukin-10, and depression-like behavior in mice after lipopolysaccharide administration. *Pharmacol Biochem Behav* **136**, 7-12 (2015).

42 Larrieu, T. & Sandi, C. Stress-Induced Depression: Is Social Rank a Predictive Risk Factor? *Bioessays* **40** (2018).

43 Zhou, Q., Yin, Z., Wu, W. & Li, N. Childhood familial environment and adulthood depression: evidence from a Chinese population-based study. *Int Health* (2019).

44 McLaughlin, K. A., Conron, K. J., Koenen, K. C. & Gilman, S. E.

Childhood adversity, adult stressful life events, and risk of past-year psychiatric disorder: a test of the stress sensitization hypothesis in a population-based sample of adults. *Psychol Med* **40**, 1647-1658 (2010).

45 Collins, S. E. Associations Between Socioeconomic Factors and Alcohol Outcomes. *Alcohol Res-Curr Rev* **38**, 83-94 (2016).

46 Butler, J. M., Whitlow, S. M., Roberts, D. A. & Maruska, K. P. Neural and behavioural correlates of repeated social defeat. *Sci Rep-Uk* **8** (2018).

47 Larrieu, T. *et al.* Hierarchical Status Predicts Behavioral Vulnerability and Nucleus Accumbens Metabolic Profile Following Chronic Social Defeat Stress. *Curr Biol* **27**, 2202-+ (2017).

48 Hare, B. D., Ghosal, S. & Duman, R. S. Rapid Acting Antidepressants in Chronic Stress Models: Molecular and Cellular Mechanisms. *Chronic Stress (Thousand Oaks)* **1** (2017).

49 Koenigs, M. & Grafman, J. The functional neuroanatomy of depression: distinct roles for ventromedial and dorsolateral prefrontal cortex. *Behav Brain Res* **201**, 239-243 (2009).

50 Liu, W. *et al.* The Role of Neural Plasticity in Depression: From Hippocampus to Prefrontal Cortex. *Neural Plast* **2017**, 6871089 (2017).

51 Duman, R. S. Ketamine and rapid-acting antidepressants: a new era in the battle against depression and suicide. *F1000Res* **7** (2018).

52 Hare, B. D. *et al.* Optogenetic stimulation of medial prefrontal cortex Drd1 neurons produces rapid and long-lasting antidepressant effects. *Nat Commun* **10**, 223 (2019).

53 Mathews, D. C., Henter, I. D. & Zarate, C. A. Targeting the glutamatergic system to treat major depressive disorder: rationale and progress to date. *Drugs* **72**, 1313-1333 (2012).

54 Chaboub, L. S. & Deneen, B. Astrocyte form and function in the developing central nervous system. *Semin Pediatr Neurol* **20**, 230-235 (2013).

55 Khakh, B. S. & Deneen, B. The Emerging Nature of Astrocyte Diversity. *Annu Rev Neurosci* **42**, 187-207, doi:10.1146/annurev-neuro-070918-050443 (2019).

56 Allen, N. J. Astrocyte regulation of synaptic behavior. *Annu Rev Cell Dev Biol* **30**, 439-463 (2014).

57 Rajkowska, G. & Stockmeier, C. A. Astrocyte pathology in major depressive disorder: insights from human postmortem brain tissue. *Curr Drug Targets* **14**, 1225-1236 (2013).

58 Banasr, M. & Duman, R. S. Glial Loss in the Prefrontal Cortex Is Sufficient to Induce Depressive-like Behaviors. *Biol Psychiat* **64**, 863-870 (2008).

59 Etievant, A. *et al.* Astroglial Control of the Antidepressant-Like Effects of

Prefrontal Cortex Deep Brain Stimulation. *Ebiomedicine* **2**, 898-908 (2015).
60 David, J. *et al.* L-alpha-amino adipic acid provokes depression-like behaviour and a stress related increase in dendritic spine density in the prelimbic cortex and hippocampus in rodents. *Behavioural Brain Research* **362**, 90-102 (2019).
61 Cobb, J. A. *et al.* Density of Gfap-Immunoreactive Astrocytes Is Decreased in Left Hippocampi in Major Depressive Disorder. *Neuroscience* **316**, 209-220 (2016).
62 Banasr, M. *et al.* Glial pathology in an animal model of depression: reversal of stress-induced cellular, metabolic and behavioral deficits by the glutamate-modulating drug riluzole. *Molecular Psychiatry* **15**, 501-511 (2010).
63 Wang, Q., Jie, W., Liu, J. H., Yang, J. M. & Gao, T. M. An astroglial basis of major depressive disorder? An overview. *Glia* **65**, 1227-1250 (2017).
64 Dossi, E., Vasile, F. & Rouach, N. Human astrocytes in the diseased brain. *Brain Res Bull* **136**, 139-156 (2018).
65 Ventorp, F. The neurobiological basis of suicide. *Acta Psychiat Scand* **128**, 495-495 (2013).
66 Xu, G. *et al.* Restraint Stress Induced Hyperpermeability and Damage of the Blood-Brain Barrier in the Amygdala of Adult Rats. *Front Mol Neurosci* **12**, 32 (2019).
67 Rajkowska, G. & Miguel-Hidalgo, J. J. Gliogenesis and glial pathology in depression. *CNS Neurol Disord Drug Targets* **6**, 219-233 (2007).
68 Duman, R. S. & Li, N. A neurotrophic hypothesis of depression: role of synaptogenesis in the actions of NMDA receptor antagonists. *Philos Trans R Soc Lond B Biol Sci* **367**, 2475-2484 (2012).
69 Davanzo, R., Copertino, M., De Cunto, A., Minen, F. & Amaddeo, A. Antidepressant drugs and breastfeeding: a review of the literature. *Breastfeed Med* **6**, 89-98 (2011).
70 Faure Walker, N., Brinchmann, K. & Batura, D. Linking the evidence between urinary retention and antipsychotic or antidepressant drugs: A systematic review. *Neurourol Urodyn* **35**, 866-874 (2016).
71 Artigas, F. Serotonin receptors involved in antidepressant effects. *Pharmacol Ther* **137**, 119-131 (2013).
72 Holck, A. *et al.* Plasma serotonin levels are associated with antidepressant response to SSRIs. *J Affect Disord* **250**, 65-70 (2019).
73 Willner, P., Hale, A. S. & Argyropoulos, S. Dopaminergic mechanism of antidepressant action in depressed patients. *J Affect Disord* **86**, 37-45 (2005).
74 Penttila, J. *et al.* Effects of fluoxetine on dopamine D2 receptors in the human brain: a positron emission tomography study with [11C]raclopride.

Int J Neuropsychopharmacol **7**, 431-439 (2004).

75 Frazer, A. Norepinephrine involvement in antidepressant action. *J Clin Psychiatry* **61 Suppl 10**, 25-30 (2000).

76 Calapai, G. *et al.* Serotonin, norepinephrine and dopamine involvement in the antidepressant action of hypericum perforatum. *Pharmacopsychiatry* **34**, 45-49 (2001).

77 Kajitani, N. *et al.* Antidepressant Acts on Astrocytes Leading to an Increase in the Expression of Neurotrophic/Growth Factors: Differential Regulation of FGF-2 by Noradrenaline. *Plos One* **7** (2012).

78 Castren, E. & Hen, R. Neuronal plasticity and antidepressant actions. *Trends in Neurosciences* **36**, 259-267, (2013).

79 Reid, I. C. Neuronal growth and synaptic plasticity: Understanding antidepressant action. *J Neurol Neurosur Ps* **72**, 828-828 (2002).

80 Castren, E. & Antila, H. Neuronal plasticity and neurotrophic factors in drug responses. *Molecular Psychiatry* **22**, 1085-1095 (2017).

81 Shirayama, Y., Chen, A. C. H., Nakagawa, S., Russell, D. S. & Duman, R. S. Brain-derived neurotrophic factor produces antidepressant effects in behavioral models of depression. *Journal of Neuroscience* **22**, 3251-3261 (2002).

82 Udo, H., Hamasu, K., Furuse, M. & Sugiyama, H. VEGF-induced antidepressant effects involve modulation of norepinephrine and serotonin systems. *Behavioural Brain Research* **275**, 107-113 (2014).

83 Martin, J. L., Magistretti, P. J. & Allaman, I. Regulation of Neurotrophic Factors and Energy Metabolism by Antidepressants in Astrocytes. *Current Drug Targets* **14**, 1308-1321 (2013).

84 Marathe, S. V., D'almeida, P. L., Virmani, G., Bathini, P. & Alberi, L. Effects of Monoamines and Antidepressants on Astrocyte Physiology: Implications for Monoamine Hypothesis of Depression. *J Exp Neurosci* **12** (2018).

85 Al-Harbi, K. S. Treatment-resistant depression: therapeutic trends, challenges, and future directions. *Patient Prefer Adher* **6**, 369-388 (2012).

86 Bennabi, L. D. *et al.* Clinical guidelines for the management of treatment-resistant depression: French recommendations from experts, the French Association for Biological Psychiatry and Neuropsychopharmacology and the fondation FondaMental. *Bmc Psychiatry* **19** (2019).

87 Tylee, A. & Walters, P. Onset of action of antidepressants. *BMJ* **334**, 911-912 (2007).

88 Machado-Vieira, R. *et al.* The Timing of Antidepressant Effects: A Comparison of Diverse Pharmacological and Somatic Treatments. *Pharmaceuticals (Basel)* **3**, 19-41 (2010).

89 Ferguson, J. M. SSRI Antidepressant Medications: Adverse Effects and

Tolerability. *Prim Care Companion J Clin Psychiatry* **3**, 22-27 (2001).
90 Wang, S. M. *et al.* Addressing the Side Effects of Contemporary Antidepressant Drugs: A Comprehensive Review. *Chonnam Med J* **54**, 101-112 (2018).
91 Boyden, E. S., Zhang, F., Bamberg, E., Nagel, G. & Deisseroth, K. Millisecond-timescale, genetically targeted optical control of neural activity. *Nat Neurosci* **8** (2005).
92 Tye, K. M. & Deisseroth, K. Optogenetic investigation of neural circuits underlying brain disease in animal models. *Nat Rev Neurosci* **13**, 251-266 (2012).
93 Hegemann, P. & Nagel, G. From channelrhodopsins to optogenetics. *Embo Mol Med* **5**, 173-176 (2013).
94 Nagel, G. *et al.* Channelrhodopsin-1: A light-gated proton channel in green algae. *Science* **296**, 2395-2398 (2002).
95 Nagel, G. *et al.* Channelrhodopsin-2, a directly light-gated cation-selective membrane channel. *P Natl Acad Sci USA* **100**, 13940-13945 (2003).
96 Armbruster, B. N., Li, X., Pausch, M. H., Herlitze, S. & Roth, B. L. Evolving the lock to fit the key to create a family of G protein-coupled receptors potently activated by an inert ligand. *Proc Natl Acad Sci U S A* **104**, 5163-5168 (2007).
97 Dong, S. Y., Rogan, S. C. & Roth, B. L. Directed molecular evolution of DREADDs: a generic approach to creating next-generation RASSLs. *Nat Protoc* **5**, 561-573 (2010).
98 Nichols, C. D. & Roth, B. L. Engineered G-protein Coupled Receptors are Powerful Tools to Investigate Biological Processes and Behaviors. *Front Mol Neurosci* **2**, 16 (2009).
99 Armbruster, B. & Roth, B. Creation of designer biogenic amine receptors via directed molecular evolution. *Neuropsychopharmacol* **30**, S265-S265 (2005).
100 Atasoy, D. Deconstruction of a neural circuit for hunger. *Acta Physiol* **217**, 10-10 (2016).
101 Krashes, M. J. *et al.* Rapid, reversible activation of AgRP neurons drives feeding behavior in mice. *J Clin Invest* **121**, 1424-1428 (2011).
102 Zink, C. F. *et al.* Know your place: neural processing of social hierarchy in humans. *Neuron* **58**, 273-283 (2008).
103 Nagy, M., Akos, Z., Biro, D. & Vicsek, T. Hierarchical group dynamics in pigeon flocks. *Nature* **464**, 890-893 (2010).
104 Sapolsky, R. M. The influence of social hierarchy on primate health. *Science* **308**, 648-652 (2005).
105 Miller, R. E. & Banks, J. H. Determination of Social Dominance in Monkeys by a Competitive Avoidance Method. *J Comp Physiol Psych* **55**,

137-& (1962).
106 Zink, C. F. *et al.* Know your place: Neural processing of social hierarchy in humans. *Neuron* **58**, 273-283 (2008).
107 Singer, T. The past, present and future of social neuroscience: A European perspective. *Neuroimage* **61**, 437-449 (2012).
108 Tan, S. *et al.* Postnatal TrkB ablation in corticolimbic interneurons induces social dominance in male mice. *P Natl Acad Sci USA* **115**, E9909-E9915 (2018).
109 Adamsky, A. *et al.* Astrocytic Activation Generates De Novo Neuronal Potentiation and Memory Enhancement. *Cell* **174**, 59-+ (2018).
110 Kronschlager, M. T. *et al.* Gliogenic LTP spreads widely in nociceptive pathways. *Science* **354**, 1144-1148 (2016).
111 Panatier, A. *et al.* Glia-derived D-serine controls NMDA receptor activity and synaptic memory. *Cell* **125**, 775-784 (2006).
112 Henneberger, C., Papouin, T., Oliet, S. H. R. & Rusakov, D. A. Long-term potentiation depends on release of D-serine from astrocytes. *Nature* **463**, 232-U120 (2010).
113 Cao, X. *et al.* Astrocyte-derived ATP modulates depressive-like behaviors. *Nat Med* **19**, 773-+ (2013).
114 Perea, G., Navarrete, M. & Araque, A. Tripartite synapses: astrocytes process and control synaptic information. *Trends in Neurosciences* **32**, 421-431 (2009).
115 Newman, E. A. New roles for astrocytes: Regulation of synaptic transmission. *Trends in Neurosciences* **26**, 536-542 (2003).
116 Navarrete, M. *et al.* Astrocytic p38alpha MAPK drives NMDA receptor-dependent long-term depression and modulates long-term memory. *Nat Commun* **10**, 2968 (2019).
117 Yang, L., Qi, Y. & Yang, Y. Astrocytes control food intake by inhibiting AGRP neuron activity via adenosine A1 receptors. *Cell Rep* **11**, 798-807 (2015).
118 Farhy-Tselnicker, I. & Allen, N. J. Astrocytes, neurons, synapses: a tripartite view on cortical circuit development. *Neural Dev* **13** (2018).
119 Chai, H. *et al.* Neural Circuit-Specialized Astrocytes: Transcriptomic, Proteomic, Morphological, and Functional Evidence. *Neuron* **95**, 531-+ (2017).
120 Fan, Z. X. *et al.* Using the tube test to measure social hierarchy in mice. *Nat Protoc* **14**, 819-831 (2019).
121 Park, M. J., Seo, B. A., Lee, B., Shin, H. S. & Kang, M. G. Stress-induced changes in social dominance are scaled by AMPA-type glutamate receptor phosphorylation in the medial prefrontal cortex. *Sci Rep-Uk* **8** (2018).
122 Stagkourakis, S. *et al.* A neural network for intermale aggression to

establish social hierarchy. *Nat Neurosci* **21**, 834-+ (2018).
123 Noh, K. *et al.* Negr1 controls adult hippocampal neurogenesis and affective behaviors. *Molecular Psychiatry* **24**, 1189-1205 (2019).
124 Lee, S. J., Zhou, T., Choi, C. H., Wang, Z. & Benveniste, E. N. Differential regulation and function of Fas expression on glial cells. *J Immunol* **164**, 1277-1285 (2000).
125 Perea, G., Yang, A., Boyden, E. S. & Sur, M. Optogenetic astrocyte activation modulates response selectivity of visual cortex neurons in vivo. *Nat Commun* **5** (2014).
126 Harada, K., Kamiya, T. & Tsuboi, T. Gliotransmitter Release from Astrocytes: Functional, Developmental, and Pathological Implications in the Brain. *Front Neurosci-Switz* **9** (2016).
127 Tada, H. *et al.* Neonatal isolation augments social dominance by altering actin dynamics in the medial prefrontal cortex. *P Natl Acad Sci USA* **113**, E7097-E7105 (2016).
128 Tatsukawa, T. *et al.* Scn2a haploinsufficient mice display a spectrum of phenotypes affecting anxiety, sociability, memory flexibility and ampakine CX516 rescues their hyperactivity. *Mol Autism* **10** (2019).
129 Ma, M. *et al.* A novel pathway regulates social hierarchy via lncRNA AtLAS and postsynaptic synapsin IIb. *Cell Res* **30**, 105-118 (2020).
130 Octeau, J. C. *et al.* Transient, Consequential Increases in Extracellular Potassium Ions Accompany Channelrhodopsin2 Excitation. *Cell Rep* **27**, 2249-+ (2019).
131 Anderson, C. & Kilduff, G. J. The Pursuit of Status in Social Groups. *Curr Dir Psychol Sci* **18**, 295-298 (2009).
132 Ferrari, A. J. *et al.* Burden of depressive disorders by country, sex, age, and year: findings from the global burden of disease study 2010. *Plos Med* **10**, e1001547 (2013).
133 Conwell, Y. *et al.* Relationships of age and axis I diagnoses in victims of completed suicide: a psychological autopsy study. *Am J Psychiatry* **153**, 1001-1008 (1996).
134 Hare, B. D. & Duman, R. S. Prefrontal cortex circuits in depression and anxiety: contribution of discrete neuronal populations and target regions. *Mol Psychiatr* (2020).
135 Warden, M. R. *et al.* A prefrontal cortex-brainstem neuronal projection that controls response to behavioural challenge. *Nature* **492**, 428-432 (2012).
136 Zhou, W. J. *et al.* A neural circuit for comorbid depressive symptoms in chronic pain (vol 22, pg 1649, 2019). *Nat Neurosci* **22**, 1945-1945 (2019).
137 de Kloet, E. R., Joels, M. & Holsboer, F. Stress and the brain: From adaptation to disease. *Nat Rev Neurosci* **6**, 463-475 (2005).
138 Pardon, M. C. & Marsden, C. A. The long-term impact of stress on brain

function: From adaptation to mental diseases. *Neurosci Biobehav R* **32**, 1071-1072 (2008).

139 Flaskerud, J. H. & DeLilly, C. R. Social determinants of health status. *Issues Ment Health Nurs* **33**, 494-497 (2012).

140 Weightman, M. J., Knight, M. J. & Baune, B. T. A systematic review of the impact of social cognitive deficits on psychosocial functioning in major depressive disorder and opportunities for therapeutic intervention. *Psychiatry Res* **274**, 195-212 (2019).

141 Kupferberg, A., Bicks, L. & Hasler, G. Social functioning in major depressive disorder. *Neurosci Biobehav Rev* **69**, 313-332 (2016).

142 Si, X. H., Miguel-Hidalgo, J. J., O'Dwyer, G., Stockmeier, C. A. & Rajkowska, G. Age-dependent reductions in the level of glial fibrillary acidic protein in the prefrontal cortex in major depression. *Neuropsychopharmacol* **29**, 2088-2096 (2004).

143 Ongur, D., Drevets, W. C. & Price, J. L. Glial reduction in the subgenual prefrontal cortex in mood disorders. *P Natl Acad Sci USA* **95**, 13290-13295 (1998).

144 Li, J. X. Pain and depression comorbidity: A preclinical perspective. *Behav Brain Res* **276**, 92-98 (2015).

145 Botia, J. A. *et al.* An additional k-means clustering step improves the biological features of WGCNA gene co-expression networks. *Bmc Systems Biology* **11** (2017).

146 Yaghouby, F. & Sunderam, S. SegWay: A simple framework for unsupervised sleep segmentation in experimental EEG recordings. *Methodsx* **3**, 144-155 (2016).

147 Dombeck, D. A., Graziano, M. S. & Tank, D. W. Functional clustering of neurons in motor cortex determined by cellular resolution imaging in awake behaving mice. *J Neurosci* **29**, 13751-13760 (2009).

148 Tseng, G. C. Penalized and weighted K-means for clustering with scattered objects and prior information in high-throughput biological data. *Bioinformatics* **23**, 2247-2255 (2007).

149 Murphy, J. M. *et al.* Depression and Anxiety in Relation to Social-Status - a Prospective Epidemiologic-Study. *Arch Gen Psychiat* **48**, 223-229 (1991).

150 Chiba, S. *et al.* Chronic restraint stress causes anxiety- and depression-like behaviors, downregulates glucocorticoid receptor expression, and attenuates glutamate release induced by brain-derived neurotrophic factor in the prefrontal cortex. *Prog Neuro-Psychoph* **39**, 112-119 (2012).

151 Gross, M., Romi, H., Miller, A. & Pinhasov, A. Social dominance predicts hippocampal glucocorticoid receptor recruitment and resilience to prenatal adversity. *Sci Rep-Uk* **8** (2018).

152 Willner, P., Daquila, P. S., Coventry, T. & Brain, P. Loss of Social-Status -

Preliminary Evaluation of a Novel Animal-Model of Depression. *J Psychopharmacol* **9**, 207-213 (1995).

153 Steinley, D. K-means clustering: A half-century synthesis. *Brit J Math Stat Psy* **59**, 1-34 (2006).

154 Steinley, D. Profiling local optima in K-means clustering: Developing a diagnostic technique. *Psychological Methods* **11**, 178-192 (2006).

155 Fuxjager, M. J. & Marler, C. A. How and why the winner effect forms: influences of contest environment and species differences. *Behav Ecol* **21**, 37-45 (2010).

156 Ferguson, B. R. & Gao, W. J. PV Interneurons: Critical Regulators of E/I Balance for Prefrontal Cortex-Dependent Behavior and Psychiatric Disorders. *Front Neural Circuit* **12** (2018).

157 Page, C. E. & Coutellier, L. Prefrontal excitatory/inhibitory balance in stress and emotional disorders: Evidence for over-inhibition. *Neurosci Biobehav R* **105**, 39-51 (2019).

158 Driessen, E. & Hollon, S. D. Cognitive Behavioral Therapy for Mood Disorders: Efficacy, Moderators and Mediators. *Psychiat Clin N Am* **33**, 537-+ (2010).

159 Passmore, T. A. & Lewy, A. J. Practice Guideline for the Treatment of Patients with Major Depressive Disorder, 2nd edition. *J Clin Psychiat* **63**, 371-371 (2002).

160 Ungvari, Z., Tarantini, S., Yabluchanskiy, A. & Csiszar, A. Potential Adverse Cardiovascular Effects of Treatment With Fluoxetine and Other Selective Serotonin Reuptake Inhibitors (SSRIs) in Patients With Geriatric Depression: Implications for Atherogenesis and Cerebromicrovascular Dysregulation. *Front Genet* **10** (2019).

국문 초록

사회 서열행동 및 우울증에 미치는 전전두엽 성상교세포의 기능 연구

서울대학교 대학원
치의과학과 신경생물학 전공
노 경 철

사회 서열에 직접적으로 관여하는 서열행동은 대부분의 동물들이 기본적으로 가지고 있는 본능행동이다. 보다 높은 사회적 위치를 달성하고 이를 유지하고자 하는 행동은 생존을 위해서 필수적이다. 최근 연구들은 뇌의 전전두엽 영역의 피라미드 신경세포가 높은 사회적 지위에 도달하고 이를 유지하는 데에 직접적인 역할을 한다는 것으로 보고하고 있다. 한편 사회적 서열과 정신 건강 사이에는 깊은 상관 관계가 있는 것으로 알려져 있는데, 낮은 사회 경제적 위치가 우울증 발병의 많은 원인 중 하나라는 연구 결과가 그 대표적이다. 뇌 전전두엽 영역의 성상교세포가 항우울제에 대한 반응에 관여하는 핵심세포로 기능하고 있는 점으로 볼 때, 성상교세포가 서열행동과 더불어 낮은 서열로 인한 우울증에 동시에 관여할 가능성이 있다. 본 연구에서는 생쥐의 서열행동과 우울증에 대한 뇌 전전두엽 성상교세포의 역할을 밝히고자 한다.

이 논문의 첫 장에서는 사회적 서열이 낮은 생쥐의 뇌 전전두엽 성상교세포를 화학 및 광유전학적으로 자극함으로써 성상교세포의 활성이 서열행동에 미치는 영향을 분석하였다. 전전두엽 성상교세포의 화학 및 광유전학적 자극은 생쥐의 저항 행동을 유발하였고, 이는 하위 서열에 있는 생쥐의 서열 상승을 크게 유도하였다. 나아가 전전두엽 성상교세포의 광유전학적 활성은 세포 밖 글루타메이트 농도를 증가 시켰으며, 이는 피라미드 신경세포로 흥분성 시냅스 입력을 증가시키는 데에 기여하였다. 더불어 서열행동을 유발하는 성상교세포와 신경세포의 차이를 확인하기 위해 성상교세포와 피라미드 신경세포를 광유전학적으로 각각 자극한 생쥐를 서로 경쟁시켰다. 그 결과 두 생쥐간의 승률은 차이가 없었지만 승리하기 위한 행동 방식이 서로 다른 것으로 나타났다.

제 2 장에서는 성상교세포 활성에 의해 유발된 서열행동이 항우울 효과를 보임을 밝혀냈다. 3 주간의 구속 스트레스를 받은 생쥐는 우울 행동을 보였을 뿐 만 아니라 급격히 저하된 서열행동을 보였다. 그러나 스트레스를 받은

생쥐의 전전두엽 성상교세포를 화학유전학적 방법으로 자극하면, 자극을 받은 생쥐는 스트레스를 받지 않은 정상 생쥐에 대하여 강한 저항 행동을 보이고, 이를 통한 반복적인 승리 이후에는 밀어내기 행동을 보였다. 이러한 행동 변화는 만성 스트레스에 의해 유발된 우울 행동을 빠르게 개선시켰는데, 피라미드 신경세포를 자극하였을 경우에는 항우울 효과가 나타나지 않았다.

본 연구에서는 생쥐의 지속적인 저항 행동으로 인한 경쟁에서의 승리가 전전두엽의 성상교세포 활성과 직접 관련이 있으며, 빠른 항우울 효과를 보인다는 것을 밝혀냈다. 이는 낮은 사회적 지위로 인해 발병하게 되는 만성 스트레스성 우울증에 대해 전전두엽의 성상교세포가 새로운 치료 타겟이 될 수 있음을 시사한다.

주요어: 서열행동, 성상교세포, 사회 서열, 전전두엽, 우울증, 항우울 효과
학번: 2014-30697